Accepted Manuscript

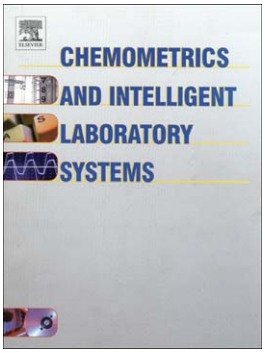

Optimization of a headspace solid-phase microextraction and gas chromatography/mass spectrometry procedure for the determination of aromatic amines in water and in polyamide spoons

L. Rubio, S. Sanllorente, L.A. Sarabia, M.C. Ortiz

PII: S0169-7439(14)00021-5
DOI: doi: 10.1016/j.chemolab.2014.01.013
Reference: CHEMOM 2761

To appear in: *Chemometrics and Intelligent Laboratory Systems*

Received date: 25 September 2013
Revised date: 20 January 2014
Accepted date: 22 January 2014

Please cite this article as: L. Rubio, S. Sanllorente, L.A. Sarabia, M.C. Ortiz, Optimization of a headspace solid-phase microextraction and gas chromatography/mass spectrometry procedure for the determination of aromatic amines in water and in polyamide spoons, *Chemometrics and Intelligent Laboratory Systems* (2014), doi: 10.1016/j.chemolab.2014.01.013

This is a PDF file of an unedited manuscript that has been accepted for publication. As a service to our customers we are providing this early version of the manuscript. The manuscript will undergo copyediting, typesetting, and review of the resulting proof before it is published in its final form. Please note that during the production process errors may be discovered which could affect the content, and all legal disclaimers that apply to the journal pertain.

ACCEPTED MANUSCRIPT

OPTIMIZATION OF A HEADSPACE SOLID-PHASE MICROEXTRACTION AND GAS CHROMATOGRAPHY/MASS SPECTROMETRY PROCEDURE FOR THE DETERMINATION OF AROMATIC AMINES IN WATER AND IN POLYAMIDE SPOONS

L. Rubio[a], S. Sanllorente[a], L.A. Sarabia[b], M.C. Ortiz[a,*]

[a]*Department of Chemistry,* [b]*Department of Mathematics and Computation*

Faculty of Sciences, University of Burgos

Plaza Misael Bañuelos s/n, 09001 Burgos (Spain)

Abbreviations[†]

Abstract

In this work, a headspace solid-phase microextraction and gas chromatography coupled with mass spectrometry (HS-SPME-GC/MS) method for trace determination of primary aromatic amines was developed. The following analytes were investigated: aniline (A), 4,4'-diaminodiphenylmethane (4,4'-MDA) and 2,4-diaminotoluene (2,4-TDA) using 3-chloro-4-fluoroaniline (3C4FA) and 2-aminobiphenyl (2ABP) as internal standards. Prior to extraction the analytes were derivatized in the aqueous solution by diazotation and subsequent iodination. The derivatives were extracted by HS-SPME using a PDMS/DVB fiber and analyzed by CG/MS. A D-optimal design was used to study the parameters affecting the HS-SPME procedure and the derivatization step. Two experimental factors at two levels and one factor at three levels were considered: (i) reaction time, (ii) extraction temperature, and (iii) extraction time in the headspace. The interaction between the extraction temperature and extraction time was considered in the proposed model. The loadings in the sample mode estimated by a PARAFAC (parallel factor analysis) decomposition for each analyte were the response used in the design because they are proportional to the amount of analyte extracted. The optimum conditions for the best extraction of the analytes were achieved when the reaction time was 20 min, the extraction temperature was 50ºC and the extraction time was 25 min. The interaction was significant.

* Corresponding author. Telephone number: 34-947-259571. *E-mail address*: mcortiz@ubu.es (M.C. Ortiz).

† Headspace solid-phase microextraction and gas chromatography coupled with mass spectrometry (HS-SPME-GC/MS), aniline (A), 4,4'-diaminodiphenylmethane (4,4'-MDA), 2,4-diaminotoluene (2,4-TDA), 3-chloro-4-fluoroaniline (3C4FA), 2-aminobiphenyl (2ABP), gas chromatography (GC), parallel factor analysis (PARAFAC), internal standard (IS), decision limit (CCα), primary aromatic amines (PAAs), World Health Organization and International Agency for Research on Cancer (WHO/IARC), Rapid Alert System for Food and Feed (RASFF), liquid chromatography-tandem mass spectrometry (LC-MS/MS), high performance liquid chromatography (HPLC), capillary zone electrophoresis (CZE), micellar electrokinetic capillary chromatography (MECC), bis-2-ethylhexylphosphate (BEHPA), isobutyl chloroformate (IBCF), solid-phase analytical derivatization (SPAD), polydimethylsiloxane/divinylbenzene (PDMS/DVB), single ion monitoring (SIM), least median of squares (LMS), capability of detection (CCβ), alternative least square (ALS), design of experiments (DOE), total ion chromatogram (TIC), core consistency diagnostic (CORCONDIA), coefficient of variation (CV).

ACCEPTED MANUSCRIPT

A calibration based on a PARAFAC decomposition provided the following values of decision limit (CCα): 1.07 μg L^{-1} for A, 1.23 μg L^{-1} for 2,4-TDA and 0.83 μg L^{-1} for 4,4'-MDA for a probability of false positive fixed at 5%. Also, the accuracy (trueness and precision) of the procedure was assessed. Furthermore, all the analytes were unequivocally identified.

Finally, the method was applied to spiked water samples and polyamide cooking utensils (spoons). 3% (w/v) acetic acid in aqueous solution was used as food simulant for testing migration from polyamide kitchenware. Detectable levels of 4,4'-diaminodiphenylmethane and aniline were found in food simulant from some of the investigated cooking utensils.

Keywords: Primary aromatic amines; HS-SPME-GC/MS; derivatization; D-optimal design; PARAFAC; migration test.

1. Introduction

Primary Aromatic Amines (PAAs) are defined as chemicals having a primary amine ($–NH_2$) attached to an aromatic ring. They range from the simplest aniline to highly complex molecules with conjugated aromatic or heterocyclic structures and multiple substituents.

Aromatic amines are extensively used in the manufacture of rubber chemical, pesticides, pharmaceuticals, dyes, photographic chemicals and as intermediates in many chemicals synthesis [1, 2]. Their major use, however, is in the production of rigid polyurethanes and polyamide. Residues of aromatic isocyanate monomers may be present in polyurethane plastics intended for food contact use. In contact with water, these isocyanates are converted to PAAs. Kitchen utensils made of nylon (the generic name for polyamides) such as turners, whisks and spoons are popularly used for cooking and frying due to their low cost, high temperature resistance and non-scratch properties. Nevertheless, chemical substances can migrate from these articles to the food, and thereby contribute to food contamination. Another example of PAAs occurrence in food packaging and their migration from polyamide utensils into foodstuffs [3,4,5] may be due to remaining residues present from the colouring process (using azo-dyes) and co-monomer addition [6,7,8].

Several PAAs have been classified as "possibly carcinogenic to humans" by the World Health Organization and International Agency for Research on Cancer (WHO/IARC) [9]. For example, 2,4-diaminotoluene (2,4-TDA) and 4,4'-diaminodiphenylmethane (4,4'-MDA) are listed in group 2B (possibly carcinogenic to humans) and aniline (A) has been classified in group 3 (not classifiable as to its carcinogenicity to humans) [10]. Hence, their presence in foodstuffs should be generally avoided. According to present legislation, European Union has set a legal limit on the permitted level of PAAs migration from materials intended to come in contact with food. As laid down by Regulation 10/2011 [11] articles intended to come in contact with food should not release PAAs above a detection level of 10 μg kg^{-1} in food or food simulant (excluding the PAAs compounds listed in Annex I Table 1 of this Regulation).

Several enforcement campaigns on PAAs have detected cases of non-compliance with EU limits in black nylon kitchen utensils. These findings are reflected in the high number of alerts on PAAs, issued by the European Commission through the Rapid Alert System for Food and

ACCEPTED MANUSCRIPT

Feed (RASFF). According to the seriousness of the risks identified and the distribution of the product on the market, the RASFF notification is classified after verification by the Commission contact point as alert, information or border rejection notification. Alert notifications are sent when a food, feed or food contact material presenting a serious risk is on the market and when immediate action is required. In the case of the risk identified does not require rapid action either because the risk is not considered serious or the product is not on the market, an information notification is sent. Commission Regulation (EU) No 16/2011 [12] has added two new sub-types of information notification: information notifications for follow-up and information for attention. A border rejection notification concerns a consignment of food, feed or food contact material that was refused entry into the Community for reason of a risk to health [13]. A total of 259 notifications were transmitted to the RASFF by different EU countries in relation to the detection of PAAs migrated from food contact materials over the last years: 21 notifications in 2005 (notification date), 16 in 2006, 17 in 2007, 29 in 2008, 51 in 2009, 35 in 2010, 33 in 2011, 41 in 2012 and 16 in the first six months of 2013 [14]. From the total of these 259 notifications, 204 were classified as alerts, 2 as information for follow-up notifications, 31 as information for attention notifications and 22 as border rejection notifications. The two main compounds identified were 4,4'-MDA and aniline. Two notifications of migration of PAAs from napkins from Germany were sent through RASFF in 2013.

Trier et al. [15] analyzed PAAs by liquid chromatography-tandem mass spectrometry (LC-MS/MS) in migrates from several samples of food-contact materials finding that unacceptably high amounts of PAAs are released by black nylon kitchen utensils to the food simulant (the 'non-detectable' limit was exceeded by up to 2100 times).

Due to their toxicity and potential carcinogenicity, determination of aromatic amines has been paid much attention and a variety of analytical procedures have been proposed for the determination of low levels of aromatic amines in various matrices [16]. Aromatic amines have already been analyzed in environmental water samples using a variety of analytical techniques such as gas chromatography (GC) coupled with different detectors [1,17,18,19], high performance liquid chromatography (HPLC) [20, 21], LC-MS/MS [15,22], capillary zone electrophoresis (CZE) [23,24], micellar electrokinetic capillary chromatography (MECC) [25] and UV-VIS spectrophotometry [26,27,28].

Amines are generally known to be very difficult to analyze with GC due to their basic character. In addition, the amino group introduces a large dipole in the molecule. This dipole is responsible for strong interaction with silanol groups and siloxane bridges in the structure of the stationary phase of the GC capillary column. This often results in non-linear adsorption effects and can be seen as strong tailing peaks in the chromatogram. The best way to prevent interaction of the strong dipole is to derivatize the amine. Derivatization of amines not only reduces the polarity but also improves the volatility, selectivity, sensitivity, and separation of them.

Greater selectivity and relatively high sensitivity of MS in combination with high separation efficiency of capillary GC can be obtained in the analysis by using GC/MS, one of the best online identification systems for the amine's peaks. Akyüz and Ata [29] proposed a GC/MS method for the determination of aliphatic and aromatic amines in a variety of environmental samples including wastewater, river water, sea water, and sediment samples. They also

ACCEPTED MANUSCRIPT

determined aromatic amines in hair dye, henna and dyed hair samples by a GC/MS method [30]. These methods include ion-pair extraction with bis-2-ethylhexylphosphate (BEHPA), derivatization of compounds with isobutyl chloroformate (IBCF) and their GC/MS analysis. Longo and Cavallaro developed a method for the determination of aromatic amines at trace levels by derivatization with heptafluorobutyric anhydride and gas chromatography electron-capture negative-ion chemical ionization mass spectrometry [31].Brede et al. developed a GC/MS method for the determination of primary aromatic amines in water samples, using solid-phase analytical derivatization (SPAD) for the sample preparation [32]. However, the GC/MS technique requires a preconcentration step to obtain good sensitivity. Muller et al. described a method for the determination of aromatic amines by SPME and GC/MS in water samples [33]. PAAs were also derivatized by diazotation and iodination and analyzed by SPE-GC/MS in Ref. [34] and by SPME-GC/MS in Ref. [35].

The following paper presents a headspace solid-phase microextraction and gas chromatography coupled with mass spectrometry (HS-SPME-GC/MS) method for trace determination of PAAs in water and in polyamide spoons. As far as the authors are aware, the literature contains no reference to the determination of PAAs by means of this HS procedure, which has the advantage that the life of the fiber is greater than in a SPME-GC/MS method. The following analytes were investigated: aniline (A), 4,4'-diaminodiphenylmethane (4,4'-MDA) and 2,4-toluenediamine (2,4-TDA) using 3-chloro-4-fluoroaniline (3C4FA) and 2-aminobiphenyl (2ABP) as internal standards (ISs). All their chemical structures appear in Table 1. Prior to extraction the analytes were derivatized in the aqueous solution by diazotation and subsequent iodination. A D-optimal design was used to study the parameters affecting the HS-SPME procedure and the derivatization step. A PARAFAC or PARAFAC2-based calibration model was carried out for each analyte (before and after the optimization step). The optimized procedure was also applied for analysing water samples and migration extracts from black nylon spoons. PARAFAC enables the unequivocal identification of aniline and its internal standard despite an interferent, which shares several m/z ions, coelutes with each of them and; therefore, the usual identification would be impossible.

2. Material and methods

2.1. Chemicals and reagents

Aniline (CAS no. 62-53-3; ACS reagent; 99.5% minimum purity), 2,4-diaminotoluene (CAS no. 95-80-7; 98% purity), 4,4'-diaminodiphenylmethane (CAS no. 101-77-9; 97% minimum purity), 3-chloro-4-fluoroaniline (CAS no. 367-21-5; 98% purity), 2-aminobiphenyl (CAS no. 90-41-5; 97% purity), hydroiodic acid (CAS no. 10034-85-2, unstabilized, 55%), sodium nitrite (CAS no. 7632-00-0; ACS reagent, 99% minimum purity), sulfamic acid (CAS no. 5329-14-6; ACS reagent; 99.3% purity) and sodium sulfite (CAS no. 7757-83-7; ACS reagent; anhydrous, 98% minimum purity) were purchased from Sigma-Aldrich (Steinheim, Germany). Sodium hydroxide (CAS no. 1310-73-2) and glacial acetic acid (CAS no. 64-19-7; HPLC grade) were obtained from Panreac (Barcelona, Spain). Methanol (CAS no. 67-56-1; for liquid chromatography LiChrosolv®) was supplied by Merck KGaA (Darmstadt, Germany).

ACCEPTED MANUSCRIPT

Deionised water was obtained by using the Milli-Q gradient A10 water purification system from Millipore (Bedford, MA, USA).

2.2. Standard solutions and samples

Stock solutions of each primary aromatic amine were individually prepared in methanol at a concentration of 500 mg L^{-1}. Intermediate solutions for each analyte at 40 mg L^{-1} were prepared by dilution with methanol. All these solutions were stored at low temperature (4ºC) and protected from light. Next, solutions of each analyte at a concentration of 400 μg L^{-1} were prepared daily in deionised water from the intermediate solutions.

The reference samples were prepared by adding the appropriate amounts of the solutions at 400 μg L^{-1} to deionised water.

Calibration standards were prepared in deionised water to each contain 0, 0.5, 1, 4, 7, 10 and 13 μg L^{-1} of the analytes (A, 2,4-TDA and 4,4'-MDA) and 1 μg L^{-1} of the two internal standards (3C4FA and 2ABP).

The samples for the optimization step were prepared in deionised water with a concentration of 7 μg L^{-1} for A, 2,4-TDA and 4,4'-MDA and 1 μg L^{-1} for the ISs.

Two water samples were analyzed. These samples were spiked with 1, 7 and 13 μg L^{-1} of A, 2,4-TDA and 4,4'-MDA. The ISs were added to all the samples at a concentration of 1 μg L^{-1}.

All the measured samples were derivatized prior to the analysis according to the procedure explained in Section 2.3.1.

Four different cooking utensils (spoons) made of black nylon and intended for contact with warm food were purchased from several local retail outlets to be tested for PAA migration.

2.3. Experimental procedure

2.3.1. Derivatization reaction

A 3 mL sample of water with the required amount of PAAs to achieve the PAAs concentration indicated in each case was placed in a 20 mL crimp-top vial of Chromacol (part of Thermo FisherScientific); then, the sample was acidified with 0.2 mL of hydroiodic acid. The solution was mixed with 0.5 mL of sodium nitrite in water (concentration 10 g L^{-1}) and shaken at 500 rpm. After a reaction time of 20 min, 1 mL of amidosulfonic acid in water (concentration 50 g L^{-1}) was added to destroy the surplus of nitrite and the mixture was shaken at 600 rpm for 45 min. The solution was heated for 5 min in a water bath at 100°C and afterwards cooled to room temperature. The surplus of iodine was destroyed with 0.25 mL of a saturated aqueous solution of sodium sulfite. The pH was adjusted to a final pH value of 8 with a solution of sodium hydroxide (5 mol L^{-1} or 10 mol L^{-1} depending on the initial pH). After that, the vials were sealed with a silicone/PTFE septum and they were stored in the refrigerator at 4ºC. Each vial was taken out of the refrigerator 50 min before its extraction with the HS-SPME procedure.

ACCEPTED MANUSCRIPT

2.3.2. Migration test conditions

Migration experiments were performed without exposure to light. Typically, kitchen utensils were too large, which is why the handle of the test specimens (four different nylon spoons) was cut. Dust was removed from the sample by wiping it with a lint-free cloth. The food simulant B [11] (3% (w/v) acetic acid in aqueous solution) was previously heated and then put into contact with the sample. Each sample was placed in a beaker and filled with 250 mL of simulant, covered with aluminium foil and transferred to a preheated oven. The top of the beaker was covered in order to reduce the loss of the simulant by evaporation. After 2 hours at 100ºC [36], the test specimens were removed from the simulant and it was cooled to room temperature. Fresh simulant was added till the original volume. Then, the simulant was stored at -20ºC until the analysis.

2.4. Instrumental

The derivatization reaction was carried out in up to 20 samples simultaneously using the magnetic stirrer GERSTEL 20 Position Twister Stir Plate (Mülheim an der Ruhr, Germany). A water bath equipped with an immersion thermostat DIGITERM 200 (JP Selecta S.A., Barcelona, Spain) with 20 L tank was employed.

Analyses were carried out on an Agilent 6890N gas chromatograph equipped with a split-splitless injector and coupled to an Agilent 5975 Mass Selective Detector (MSD) from Agilent technologies. Chromatographic separation was achieved with the J&W DB-5MS capillary column with dimensions of 30 m × 0.25 mm I.D, 0.25 μm film thickness (J&W Scientific, Folsom, CA, USA).

The HS-SPME procedure was performed using a Triplus autosampler equipped with an SPME module (Thermo Scientific, Milan, Italy) controlled by means of the software Triplus Sampler version 1.6.9 SPME (Thermo). A glass liner for SPME (0.75 mm I.D) and a polydimethylsiloxane/divinylbenzene fiber (PDMS/DVB, 65 μm film thickness) from Supelco (Bellefonte, PA, USA) were used. The fibers were conditioned, before their first use, according to the recommendations of the manufacturer (250ºC, 30 min).

2.5. Parameters of HS-SPME and GC/MS conditions

The derivatized analytes were extracted from the aqueous matrices by HS-SPME and finally determined by GC/MS. For the HS-SPME procedure, extraction was carried out with agitation. The vials were placed in a shaker bath with a constant temperature (extraction temperature: 50ºC) and they were shaked during 25 s followed by 5 s in rest. Samples were incubated for 5 min and, then, the fiber was exposed to the headspace over the sample for 25 min (extraction time). However, the extraction time was 30 min for the samples analyzed before the optimization step. The sampling vial depth was fixed at 20 mm. After this period, the fiber was immediately inserted into the hot injector of the GC for desorption. The fiber was desorbed for 2 min at 250ºC. The depth of penetration of the needle in the injector port was 35 mm. The conditioning of the fiber took place for 15 min at 250ºC.

ACCEPTED MANUSCRIPT

Injections were performed in splitless mode with the split valve closed for 2 min. The injector was kept at the temperature of 250ºC. The oven temperature was maintained at 50ºC for 2 min needed for the fiber desorption. Then, the temperature was increased at 20ºC min^{-1} until 180ºC (2 min). The second ramp was programmed from 180 to 290ºC with a heating rate of 50ºC min^{-1}, and held at this temperature for 3 min. A post-run of 3 min at 290ºC was established. The oven equilibration time was set to 0.25 min.

Helium was used as the carrier gas at a constant flow rate of 2 mL min^{-1}.

After 5 min (solvent delay), the mass spectrometer was operated in the electron impact (EI) ionization mode at 70 eV operating in single ion monitoring (SIM) mode. The transfer line temperature was set at 300ºC, the ion source temperature at 230ºC and the quadrupole temperature at 150ºC.

Five groups of *m/z* ratios, were acquired in SIM mode. For A (group 1) the *m/z* ratios recorded were 50, 51, 77, 127 and 204. For 3C4FA (group 2, start time: 6.5 min), the following ion fragments were selected: 109, 127, 129, 163, 256, 258 and 295. In this case, the *m/z* ratios 163 and 295 were taken into account for modelling the interferent. For 2,4-TDA (group 3, start time: 7.5 min), the *m/z* ratios were 90, 127, 202, 217, 329 and 344. For 2ABP (group 4, start time: 10 min) the *m/z* ratios recorded were 76, 127, 151, 152, 153 and 280. And for 4,4´-MDA (group 5, start time: 11.5 min), 90, 165, 217, 293 and 420 were selected as ions. The diagnostic ions can be seen in the last column of Table 1.The dwell time per *m/z* ratio was 30 ms.

2.6. Software

MSD ChemStation version E.02.00.275 (Agilent Technologies, Inc.) with Data Analysis software were used for data acquisition and processing as well as the NIST mass spectral library [37]. Data tensors were constructed with MATLAB version 7.10 (The MathWorks, Inc.). PARAFAC and PARAFAC2 models were computed with PLS Toolbox 6.0.1 [38] for use with MATLAB. NEMRODW [39] was employed for the selection and analysis of the D-optimal design. The linear regression models were built and validated with STATGRAPHICS Centurion XVI [40] and the outliers detection in the regression models was carried out with PROGRESS [41] that implements least median of squares (LMS) regression. Decision limit ($CC\alpha$) and capability of detection ($CC\beta$) were determined using the DETARCHI program [42].

3. Theory

3.1. D-optimal design

The methodology based on the design of experiments (DOE) is a useful tool that might be employed for finding the best experimental conditions.

ACCEPTED MANUSCRIPT

In this work, the derivatization reaction and the analysis are time-consuming. Each individual experiment needs approximately one hour of analysis. Moreover, we want to perform two replicates of an experiment. The number of experiments must be reduced so that the experimental plan can be performed on the same day. Since it is not possible to carry out more than 12 experiments in a day, the experiments to be performed were selected according to the D-optimality criterion. A D-optimal design enables to reduce the experimental effort to that strictly necessary to estimate all the effects and the interaction of interest with enough precision.

Briefly, the steps in the selection of the design were as follows and complete details can be seen in reference [43]:

(i) First step: Define the factors to be analysed and their levels establishing all the possible candidate N_C experiments. In this work, the effect of three experimental factors has been evaluated. Two of them (reaction time and extraction temperature) were at two levels, whereas the other factor (extraction time in the headspace) was at three levels because we considered that its effect on the response will not be linear due to previous experiences. The interaction between the extraction temperature and the extraction time has been also taken into account. Table 2 shows the factors under consideration and their levels. The candidate experiments were those required for the performance of the complete factorial design (12 experiences). In our case, it was only possible to perform a maximum of 10 experiments of the design considering the analysis time and the two replicates we wanted to carry out. The number of experiments was reduced by means of a D-optimal design.

(ii) Second step: Propose a model and in particular establish the number of its coefficients (p). In this case, the mathematical reference-state model [43] can be expressed as follows:

$$y = \beta_0 + \beta_{1A} x_{1A} + \beta_{2A} x_{2A} + \beta_{3A} x_{3A} + \beta_{3B} x_{3B} + \beta_{2A3A} x_{2A} x_{3A} + \beta_{2A3B} x_{2A} x_{3B} + \varepsilon \quad (1)$$

The highest level was considered as the reference level for all the factors of the model (level C for the third factor and level B for the rest). Variables x_{ij} of model of Eq. (1) take the value of 1 when the factor *'i'* is at the level which is written in the subscript '*j*', and they take the value of 0 when the factor *'i'* is at other different level of *'j'*. The coefficient β_{iA}, i =1, 2, is the variation of the response when the factor *'i'* changes from level B to level A. In the particular case of the 3-level factor (factor 3), β_{3A} means the variation of the response when that factor moves from level C to level A, and β_{3B} that when it does to level B. These coefficients can be estimated by least squares. Interactions are described by the products of the corresponding variables. Since there are 7 coefficients in the model, at least 7 experiments extracted from the complete factorial design are necessary to fit the model.

(iii) Third step: Verify the coherence between the model and the information obtained in the candidate points. Considering the complete factorial design, the value for the variance inflation factor (VIF) was 1 for β_{1A} and β_{2A} and 1.33 for the rest of the coefficients.

(iv) Fourth step: Construct various experimental matrices with information of sufficiently good quality for different values of the number of experiments, *N*. *N* vary between the minimum value possible (p) and value smaller or equal to N_C. In other words, for each *N* between 7 and 12 the *N* experiments which give the best estimation of the coefficients (minimum

ACCEPTED MANUSCRIPT

volume of confidence ellipsoid) are determined. For each *N*, the election of the *N* experiments from the full factorial design is done through an exchange algorithm [43].The final number of experiments of the D-optimal design was chosen in such a way that the maximum of the VIFs was close to 1 to guarantee sufficiently precise estimations for the coefficients of the model. The selected design, for which a first minimum of the maximum VIF was reached (maximum VIF = 1.2), had 10 experiments. Table 3 shows the D-optimal design chosen with 10 experiments (plus 2 replicates: experiments 10 and 11 are replicates of experiment 9).

3.2. PARAFAC and PARAFAC2 decompositions

GC/MS data are arranged in a three-way array, **X**, and analyzed with the three-way decomposition techniques PARAFAC or PARAFAC2. In this section, the parallelism that exists between the PARAFAC decomposition and a physical model of GC/MS data, under some common assumptions, is described.

Considering an analyte, its abundance x_j recorded by a MS spectrometer at the *j*th *m/z* ratio is

$$x_j = \varepsilon_j \chi, \qquad j = 1, 2, \ldots, J \tag{2}$$

where ε_j is a coefficient of proportionality between the analyte concentration and the abundance. ε_j depends on the *j*th *m/z* ratio; the vector of these coefficients constitutes the spectral profile (related to the mass spectrum).

As the mass spectrometer is coupled to a chromatograph, the signal (abundance) not only depends on the *m/z* ratio and the concentration of the analyte but also on the elution time, because the fraction of analyte that is eluting from the chromatographic column to the mass spectrometer, changes over time. So at the *i*th elution time, the recorded abundance becomes

$$x_{ij} = \tau_i \varepsilon_j \chi, \qquad i = 1, 2, \ldots, I;\ j = 1, 2, \ldots, J \tag{3}$$

where τ_i can be considered as the fraction of analyte that is going through the mass spectrometer at time *i*. The vector of all τ_i forms the chromatographic profile (related to the chromatographic peak).

If *F* spectrally active substances coelute, the recorded abundance is the sum of the contributions of these *F* different compounds

$$x_{ij} \cong \sum_{f=1}^{F} \tau_{if} \varepsilon_{jf} \chi_f, \qquad i = 1, 2, \ldots, I;\ j = 1, 2, \ldots, J \tag{4}$$

Finally, assuming that analyte *f*th has the same retention time in all chromatographic runs, the abundance measured at the *j*th *m/z* ratio, the *i*th retention time and the *k*th sample can be expressed as

ACCEPTED MANUSCRIPT

$$x_{ijk} \cong \sum_{f=1}^{F} \tau_{if} \varepsilon_{jf} \chi_{kf} \ , \quad i = 1, 2,\ldots, I; \quad j = 1, 2,\ldots, J; \quad k = 1, 2, \ldots, K \tag{5}$$

The set of all x_{ijk} data forms the three-way array **X**.

A PARAFAC model of rank *F* can be expressed [44,45] as

$$x_{ijk} = \sum_{f=1}^{F} a_{if} b_{jf} c_{kf} + e_{ijk} \ , \quad i = 1, 2,\ldots, I; \quad j = 1, 2,\ldots, J; \quad k = 1, 2, \ldots, K \tag{6}$$

where e_{ijk} are the residuals of the model. As can be observed, the PARAFAC model of Eq. (6) corresponds to the physical model of Eq. (5).

Under the above-mentioned conditions, a PARAFAC model of *F* components can be used to estimate the coefficients of proportionality for each analyte at all *m/z* ratios recorded (i.e. the mass spectral profile of each analyte) by means of vector $\mathbf{b}_f = (b_{1f}, b_{2f}, \ldots, b_{Jf})$; the fraction of analyte that leaves the chromatographic column along the chromatographic run (i.e. the chromatographic profile or chromatogram of the analyte) by means of the vector $\mathbf{a}_f = (a_{1f}, a_{2f}, \ldots, a_{If})$; and the relative concentration of every analyte in all k samples (i.e. the sample profile of each analyte) by means of the vector $\mathbf{c}_f = (c_{1f}, c_{2f}, \ldots, c_{Kf})$. The coordinates of vectors $\mathbf{a}_f$, $\mathbf{b}_f$ and $\mathbf{c}_f$ are respectively referred to as chromatographic, spectral and sample loadings and are the columns of matrix **A**, **B** and **C** of size $I \times F$, $J \times F$ and $K \times F$ respectively.

Equation (6) shows that the PARAFAC model is trilinear, that is, it is linear in each of the three modes (profiles). Moreover, the product is a commutative operation so the profiles can be exchanged without modifying the model. The PARAFAC model allows to describe each of the slabs ($\mathbf{X}_k$, k=1,2,…, K) that form the tensor **X** by the following equation

$$\mathbf{X}_k = \mathbf{A}\mathbf{D}_k\mathbf{B}^t + \mathbf{E}_k \ , \quad k = 1, 2, \ldots, K \tag{7}$$

where **A** and **B** are already defined**,** $\mathbf{D}_k$ is a diagonal $F \times F$ matrix containing the *k*th row of **C** matrix and E denotes an $I \times J$ matrix with residuals not modelled by PARAFAC. It is clear in Eq. (7) that the chromatographic and spectral profiles are the same in all the samples. Therefore, a slab (matrix of abundances recorded for each chromatographic run) of the data tensor **X** differs from another slab only in the proportion of each factor; that is, in the concentration of each compound.

The PARAFAC model is unique under relatively mild conditions and is highly affected by deviations from the trilinear structure. A frequent problem that affects trilinearity is the changes in the retention time of the different analytes between runs, which means that the correct physical model for *k*th sample is the following:

ACCEPTED MANUSCRIPT

$$\underline{\mathbf{X}} = \left(x_{ijk}\right) = \left(\sum_{f=1}^{F} a_{if}^{k} b_{jf} c_{kf} + e_{ijk}\right), \quad i = 1, 2, \ldots, I; \quad j = 1, 2, \ldots, J; \quad k = 1, 2, \ldots, K \tag{8}$$

where the superscript (*k*) is added to account for the dependence of the chromatographic profile on the sample. In this case, each slab of the tensor will be written as

$$\mathbf{X}_k = \mathbf{A}_k \mathbf{D}_k \mathbf{B}^t + \mathbf{E}_k, \quad k = 1, 2, \ldots, K \tag{9}$$

because there is a chromatographic profile different for each sample. The matrices and residuals of this model are different from the ones in model of Eq. (7), despite the notation remains the same to indicate that they should ideally be equal. The model of Eq. (9) does not have the uniqueness property. To recover it, Harshman [46] imposed the constraint that the cross product $\mathbf{A}_k{}^t \mathbf{A}_k$ is constant over *k*. In addition, Kiers et al. [47] provide simulation results suggesting that the direct fitting PARAFAC2 solutions seems to be unique whenever $K \geq 4$ for any value of *F*.

The PARAFAC2 decomposition technique, whose equation corresponds to (8) and (9), overcomes the inequality in the chromatographic profiles and allows some deviation in them [48].

When mass spectrometry is used as detector it is normal to work in SIM mode at different m/z ratios for each analyte because the sensitivity is better that in full scan mode. Therefore, in target analysis PARAFAC (or PARAFAC2) decomposition must be done for each chromatographic peak separately [49]. This makes it easier, in practice, compliance with the equality constraint about the cross product matrices [48].

The PARAFAC model has been fitted by means of the alternative least square (ALS) algorithm and PARAFAC2 by the direct fitting algorithm [47]. In addition, it is possible to impose realistic and appropriate restrictions on the model with PARAFAC (or PARAFAC2) decompositions, such as non-negativity (which is appropriate for the chromatographic or spectral profiles) or the unimodality property (which is appropriate for the chromatographic profile).

Both models, PARAFAC and PARAFAC2, can be applied to chromatographic-mass spectrometry data and both of them have the uniqueness property that is key to the unequivocal identification. But both models have benefits and drawbacks. It is true that PARAFAC give more robust models, particularly because in PARAFAC the number of parameters to be estimated, $(I + J + K) \times F$, is far less than in PARAFAC2, $(I \times K + J + K) \times F$. Therefore the former one can handle noise much better than the latter. Nevertheless, the trilinearity constraint in PARAFAC makes the use of PARAFAC2 indispensable in some other cases because the cross-product constraint is less restrictive.

Therefore, given an experimental tensor $\underline{\mathbf{X}}$, it is necessary to decide which of the two models fit better the GC/MS data. Initially, a PARAFAC model is fitted and its validation is performed by means of the variance explained and the core consistency diagnostic (CORCONDIA), developed by Bro and Kiers [50]. If the data tensor is trilinear, then the maximum

ACCEPTED MANUSCRIPT

CORCONDIA value of 100 is found. The coherence of loadings with the experimental knowledge is also investigated. The accepted way to compare two profiles (two columns of matrices **A**, **B** or **C**); for example, $\mathbf{a}_f$ and $\mathbf{a}_l$, is via the cosine of the angle between them

$$cos\left(\mathbf{a}_f, \mathbf{a}_l\right) = \frac{\sum_{j=1}^{J} a_{jf} a_{jl}}{\sqrt{\sum_{j=1}^{J} a_{jf}^2} \sqrt{\sum_{j=1}^{J} a_{jl}^2}} \quad (10)$$

If two factors have the same spectral and sample profiles but different chromatographic profile, it can be concluded that the same compound at the same quantities in the samples elutes at different times. In this case, the PARAFAC model is not coherent with the experimental data tensor because each chromatographic peak is analyzed separately and therefore we expect only, in the same peak, other compounds with different spectra. Haven and ten Berge [51] have found that factors are judged as being "virtually equal" whenever the cosine for the loadings of two factors is above 0.85. A later study [52] suggests that a value in the range 0.85-0.94 corresponds to fair similarity, while a value higher than 0.95 implies that the two factors compared can be considered equal.

If the PARAFAC model is not suitable for the data tensor **X** then proceeds to use a PARAFAC2 model. Together with the variance explained, a model diagnostic similar to core consistency for PARAFAC2 models recently developed [53] can be applied.

Like in two-way data based calibration methods, one can diagnose whether the PARAFAC-based calibration model is suitable for a specific sample by the "*ad hoc"* versions of the Q and T^2 statistics for each mode. This makes it possible to detect anomalies in the experimental data used in the construction of models and also to avoid the incorrect application of the calibration model to a sample different from those used in fitting the calibration model.

We have already discussed the need to use PARAFAC2 to correct deviations in retention times. It must be remembered that this will not be a very marked problem in regulated analysis, since working conditions are required such that the possible shift of the retention time is limited. In [54] it is established that the relative retention time of the analyte shall correspond to that of the calibration solution at a tolerance of ±0.5% for GC.

4. Results and discussion

4.1. Tolerance intervals for the unequivocal identification of the analytes

Commission Decision 2002/657/CE [54] establishes requirements for the unequivocal identification of the analytes. In the specific case of migrants [55], the requirements remain the same as the above mentioned Decision. This identification in GC/MS will be carried out according to the relative retention time and the mass spectrum recorded in *full scan* or in SIM mode. These documents state that it is necessary to verify that: (i) the relative retention time (the ratio of the chromatographic retention time of the analyte to the retention time of its internal standard) corresponds to that one of a reference sample within a tolerance margin of

ACCEPTED MANUSCRIPT

± 0.5% and (ii) the relative abundances of the recorded ions for each analyte shall be within the maximum permitted tolerances calculated using a reference sample and expressed as a percentage of the intensity of the base peak. Both documents establish that for the detection using mass spectrometry in SIM mode, the molecular ion shall preferably be one of the selected diagnostic ions (provided it is stable) together with other characteristic fragment ions and all its isotope ions. Table 1 contains the selected ions for each iodinated derivative. The fragment *m/z* 127, corresponding to the iodine substituent, has been selected in several of the derivatives despite its intensity is low.

In this work, eight reference samples were used to establish the permitted tolerance intervals: three of them at a fixed concentration (7 μg L^{-1}) of the three analytes (A, 2,4-TDA and 4,4'-MDA) and the internal standards (3C4FA and 2ABP) at three different levels of concentration (1, 2 and 3 μg L^{-1}), another three samples contained the internal standards at a fixed concentration (1 μg L^{-1}) and the analytes at three different levels of concentration (1, 7 and 13 μg L^{-1}); while the two remaining samples were replicates of the samples that contained 1 and 13 μg L^{-1} of the analytes and 1 μg L^{-1} of the internal standards. An empty headspace vial and two reagent blank samples were measured at the beginning. Fig. 1 shows the total ion chromatograms (TIC) superimposed of some of these samples. The analytes do not appear in the sample corresponding to the empty headspace vial measured. Taking the concentrations of the samples into account, it is observed that the peaks corresponding to the analytes increase in a coherent way, except for 3C4FA due to the abundance of this analyte is masked by an interferent.

The experimental data, obtained from these samples, were distributed in data tensors **X**. To build these tensors, the chromatograms were fragmented around the retention time in which the maximum abundance is obtained for each of the analytes after baseline correction for each case. Next, the matrices obtained for each sample were arranged together to form **X**. Table 4 shows the size of the data tensors built in this section for each of the 5 compounds (column 4). A PARAFAC model was performed for each of the tensors with the non-negativity constraint imposed for the three ways.

In the case of aniline, as can been seen in Fig. 1, an interferent appears on the right side of this analyte peak so 13 scans were only considered to minimize its effect. The first row of Table 5 shows the analysis followed, after fitting a one-factor PARAFAC model, to obtain an adequate decomposition. Firstly, it is evaluated whether there is still effect of the interferent in the tensor. To do this, a two-factor PARAFAC model is fitted (the profiles of these two PARAFAC models are shown graphically in the Electronic Supplementary Material, Fig. S1). The cosines of the angles that form the loadings of the two factors show that there is a unique sample and spectral profile; therefore, there is only an analyte despite having two chromatographic profiles. This fact suggests the possibility of shifts in the chromatographic profile. Thus, a one-factor PARAFAC2 model was fitted. This model explains a variance percentage higher than in PARAFAC. The cosine of the spectral loading vector in both models, PARAFAC and PARAFAC2, is 0.9999 and the value of the cosine for the sample mode is 0.9998; as a result, it can be concluded that both models identify the same analyte in the same quantity. Fig. 2a shows the chromatographic profile obtained in the PARAFAC model in which the maximum loading is reached at the elution time of 5.553 min. Fig. 2b shows the results obtained with PARAFAC2, a chromatographic profile for each sample, in

ACCEPTED MANUSCRIPT

which the highest loadings are reached at 5.550 min. (one sample), 5.553 min. (one sample), 5.555 min. (four samples) and 5.558 (one sample); that is, the difference between the retention times is at most 0.008 min. and this value is admissible according to the permitted tolerances. Therefore, both models would be valid to describe the data tensor and to unequivocally identify the aniline with the spectral and chromatographic profile. The increase of 2.5% of the explained variance justifies choosing a one-factor PARAFAC2 model for the data tensor of aniline.

When the Q and T^2 statistics were applied, the penultimate sample of the one-factor PARAFAC2 model (which contained 13 $\mu g\ L^{-1}$ and 1 $\mu g\ L^{-1}$ of the internal standards) was considered an outlier.

For 2,4-TDA, 2ABP and 4,4'-MDA, the PARAFAC model required just one factor. However, the PARAFAC model for 3C4FA needed two factors: the former one related to an interferent. The abundance of this interferent is greater than the abundance of the derivatized analyte at the studied concentrations. The *m/z* ratios 163 and 295 recorded are characteristic of the interferent and help to model it. All the ions recorded for 3C4FA were also shared with this coeluting compound. The interferent has been separated perfectly from the analyte in that model. It was checked that there were not outlier data in these last models. Table 4 shows some characteristics of the models built.

PARAFAC and PARAFAC2 decompositions provide a unique spectral profile for each analyte that is common to all the samples. The spectral loadings obtained in these decompositions were used to calculate the relative abundances of each *m/z* ion recorded with respect to the base peak and thus determine the permitted tolerance intervals for each ion according to regulations [54,55]. These tolerance intervals are shown in the fourth column of Table 6.

To ensure the unequivocal identification, the tolerances for the relative retention time of each analyte were also estimated. The retention time obtained through PARAFAC model is the one corresponding to the "scan" with the largest loading on the chromatographic profile that is common in all samples. These values obtained for each analyte are collected in the sixth column of Table 1. However, in PARAFAC2 a scan is selected in the range of the highest loadings (see Fig. 2b), for example 5.555 min for aniline.

4.2. Calibration before the optimization step

A calibration at seven levels of concentration (0, 0.5, 1, 4, 7, 10 and 13 $\mu g\ L^{-1}$) of the analytes (A, 2,4-TDA and 4,4'-MDA) was performed in order to compare the figures of merit that will be obtained in this case with the ones of the calibration that will be performed in optimal conditions. An empty headspace vial was measured before this calibration to verify that memory effect does not exist in the fiber used. All the samples contained 1 $\mu g\ L^{-1}$ of the internal standards (3C4FA and 2ABP).

To carry out the calibration based on PARAFAC or PARAFAC2, the data tensors were built with these samples. The sample corresponding to the empty headspace vial was included in these data tensors for the decomposition but it will not be used for calibration. The

ACCEPTED MANUSCRIPT

dimension of the data tensors and some characteristics of the PARAFAC or PARAFAC2 models performed are shown in Table 4. For aniline, an analysis similar to that of section 4.1 is shown in the second row of Table 5. The PARAFAC model with two factors has the same spectral and sample loadings in both factors but different chromatographic profile. The PARAFAC and PARAFAC2 models with one factor have the same spectral (cosine equal to 1) and sample profile (cosine equal 1). As in Section 4.1, it was decided to use the PARAFAC2 model.

Again, the PARAFAC decomposition of 3C4FA needed two factors. The chromatographic, spectral and sample profiles of this analyte and of the compound that coelutes with it are shown in Fig. 3. In Fig. 3 (a), it is clearly seen the difference in abundance between both compounds and that the analyte peak is completely overlapped with that of the interferent, which shows the complexity of the problem. In Fig. 3 (b) it can be observed that the characteristic *m/z* ratios of the interferent (*m/z* 163 and 295) do not appear in the spectral profile of the analyte, as expected. On the other hand, all the *m/z* ratios of the analyte are shared with the coeluting compound. The loadings of the sample mode (Fig. 3 (c)) are coherent and they remain almost constant for the interferent. It is possible that this interferent may be present in the instrument and/or in the fiber since it appears in the first sample (the one corresponding to the empty headspace vial, see Fig. 3 (c)). There is not memory effect (for the target analyte) because the sample corresponding to the empty headspace vial has null value of the sample loading for 3C4FA.

For all the analytes, it was checked if the relative loadings of the spectral profile, 5th column in Table 6, were within the tolerance intervals established previously in Section 4.1 (4th column, Table 6). The identification is correct according to regulations because 3 *m/z* ratios were compliant. Furthermore, it was verified that the relative retention time for the analytes does not exceed $\pm$ 0.5% the relative retention time of the reference samples. Therefore, the analytes were unequivocally identified.

Subsequently, the loadings of the sample mode for each analyte were standardized by dividing each loading by the corresponding of its internal standard. A least squares (LS) regression model "standardized loading *versus* true concentration" was performed for each analyte. The sample that contained 10 μg L^{-1} was removed from the regressions for 2,4-TDA and 4,4'-MDA because it was considered an outlier. These regressions were significant in all cases. Next, the accuracy line is performed. At a significance level of 0.05, the intercept was equal to 0 and the slope was equal to 1; thus the trueness was fulfilled, that is, there was neither constant nor proportional bias, and the precision was adequate. The results of this analysis together with some validation parameters are collected in Table 7. The values of the decision limit (CCα), for a probability of false positive (α) equal to 0.05, were 1.66 μg L^{-1} for A, 1.74 μg L^{-1} for 2,4-TDA and 2.36 μg L^{-1} for 4,4´-MDA; while the values of the capability of detection (CCβ), for probabilities of false positive and false negative (β) fixed at 0.05, were 3.18 μg L^{-1}, 3.32 μg L^{-1} and 4.51 μg L^{-1}, respectively. The details of the procedure to obtain capability of detection (CCβ) can be consulted in Ref. [56] for calibrations with first-order data and in [57] with second-order data.

4.3. Optimization of the HS-SPME procedure and of the derivatization reaction

ACCEPTED MANUSCRIPT

To increase the amount of analyte extracted by the fiber, some of the parameters corresponding to the HS-SPME procedure and to the derivatization reaction were optimized using a D-optimal design. Specifically, three parameters were studied: two of them affect the HS-SPME procedure (extraction time and extraction temperature) and the other one affects the derivatization step (reaction time). Table 2 shows the levels of the factors. The procedure of selection of this D-optimal design can be consulted in Section 3.1.

Given that the procedure includes a HS-SPME step, it was not possible to analyze the same sample repeatedly, unlike in liquid injection. Therefore, twelve samples that contained 7 $\mu g\ L^{-1}$ of A, 2,4-TDA and 4,4'-MDA with 1 $\mu g\ L^{-1}$ of the internal standards were derivatized and measured according to the experimental plan (see Table 3). A reagent blank sample and two empty headspace vials (one at the beginning and the other at the end of the analysis) were also measured, in the same conditions used at the moment (the ones of the experiment 9) to verify that the fiber was clean before conducting the next measurement. There was not memory effect of the analyte.

The analysis of the tensor of aniline, as can be seen in the third row of Table 5, indicates that the PARAFAC model with two factors has the same structure as in the two previous cases (reference samples and calibration before the optimization step). When the profiles of the PARAFAC and PARAFAC2 models with one factor are compared, the values of the cosines are 1 and 0.998 for the spectral and sample mode, respectively. As in the previous cases, the PARAFAC2 model was chosen because it explained more variance. It is remarkable the similarity of PARAFAC2 and PARAFAC models for the three aniline data tensors as can be seen in Table 5.

The PARAFAC models for 2,4-TDA, 2ABP and 4,4´-MDA needed just one factor.

For 3C4FA, it was necessary to add three additional samples to its data tensor to obtain an adequate PARAFAC model. Specifically, the added samples contained different amounts of 3C4FA because PARAFAC needs a greater variation of this analyte (internal standard), which is masked by the abundance of its interferent, to model correctly. Two of the added samples contained 10 $\mu g\ L^{-1}$ of 2,4-TDA, 2ABP and 4,4'-MDA, while the other contained 7 $\mu g\ L^{-1}$ of these analytes. The concentration of the internal standards in these samples was 10, 0.5 and 5 $\mu g\ L^{-1}$, respectively. In this case, the PARAFAC models do not fit the data tensors. It is know that an interferent coelutes with 3C4FA but the PARAFAC model with 2 factors has a small CORCONDIA index (19%) and explains the 99.47% of variance. Moreover, the cosines between the two factors are 0.4611, 0.9964 and 0.6543 for the chromatographic, spectral and sample profiles, respectively. These values suggest only one compound instead of the two expected compounds. The CORCONDIA index for the PARAFAC model with 3 factors is negative so it is not adequate. Nevertheless, the two-factor PARAFAC2 model, showed in Table 4, has a CORCONDIA index of 100%.

No outlier data were found at the 99% confidence level taking into account the Q and T^2 statistics. Some characteristics of those models can be consulted in Table 4. The unequivocal identification was guaranteed in all cases.

The loadings of the sample profile for each experiment constituted the responses considered for the analysis of the design (columns 5-9 of Table 3) because they were proportional to the

ACCEPTED MANUSCRIPT

amount of analyte that has been extracted by the fiber. In the case of aniline and 3C4FA, these loadings were numerically high because the way that is not normalized in the PARAFAC2 decomposition is the third (sample profile in this case). The loadings were used to fit the model of Eq. (1) for each of the five compounds. Some data, marked with an asterisk in Table 3, were considered outliers for the corresponding model. However, there are enough degrees of freedom to evaluate the significance of all the models and of the coefficients and to test the lack of fit. All of them were significant at the 93% confidence level. It is also possible to conclude that there was not lack of fit at the 95% confidence level, since the p-value of the corresponding hypothesis test was higher than 0.05. Depending on the analyte, the values of determination coefficient (R^2) ranged from 0.95 to 0.98.

The coefficients of the reference-state model of Eq. (1) are estimated by least squares; however, that model was converted into the equivalent presence-absence model of Eq. (11) with coefficients β' for an easier interpretation of the effect of the experimental factors.

$$y = \beta'_0 + \beta'_{1A} x_{1A} + \beta'_{1B} x_{1B} + \beta'_{2A} x_{2A} + \beta'_{2B} x_{2B} + \beta'_{3A} x_{3A} + \beta'_{3B} x_{3B} + \beta'_{3C} x_{3C} + \beta'_{2A3A} x_{2A} x_{3A} + \beta'_{2A3B} x_{2A} x_{3B} + \beta'_{2A3C} x_{2A} x_{3C} + \beta'_{2B3A} x_{2B} x_{3A} + \beta'_{2B3B} x_{2B} x_{3B} + \beta'_{2B3C} x_{2B} x_{3C} + \varepsilon \quad (11)$$

In Eq. (11) each coefficient β'_{fL}, f = 1,..3; L = A, B or C, is the effect in the response when the factor f is at level L. There is a relation between the coefficients β of the reference-state model and β' of the presence-absence model, so once the coefficients of Eq. (1) are estimated, the ones of Eq. (11) can be obtained [43].

Fig. 4 shows graphically the estimated coefficients of Eq. (11). The factors and their corresponding levels are detailed in Table 2. Since the aim of the design is to obtain maximum extraction of the analytes, the optimal conditions will be those in which the significant factors have a positive coefficient. The factor 1 (reaction time) was not significant in any case so the reaction time was fixed at the shortest time studied (20 min). The factor 2 (extraction temperature) was not significant for 2,4-TDA and 2ABP, whereas it was for the rest of the analytes. In this case, the optimal temperature for 4,4'-MDA was 65ºC, while for aniline and 3C4FA it was 50ºC. The third factor (extraction time) was significant in all cases but there was also a conflict when choosing the optimal time, since it was 25 min for aniline and 3C4FA and 30 min for the rest. The interaction was significant in all cases except for 2,4-TDA and it was coherent with the principal effect of the factors evaluated above for each case. Taking into account that an interferent coelutes with aniline and another with 3C4FA in this work, the conditions were selected with the aim of improving the signal of both analytes. Therefore, the optimal conditions were: reaction time (20 min), extraction temperature (50ºC) and extraction time (25 min).

4.4. Validation of the analytical procedure

4.4.1. Calculation of the figures of merit

ACCEPTED MANUSCRIPT

A new calibration was performed in the optimal conditions obtained in Section 4.3, for the validation of the analytical procedure and to calculate the figures of merit. To do this, the same calibration range as the one in Section 4.2 was prepared. Three levels of concentration (1, 7 and 13 μg L^{-1}) were replicated. Furthermore, six calibration standards spiked at 7 μg L^{-1} were prepared to evaluate the repeatability of the procedure. Likewise, two empty headspace vials were measured: the former at the beginning of the calibration and the other at the end of the measurement of the repeatability samples to study the memory effect of the fiber. The concentration of the two internal standards was 1 μg L^{-1} in all the samples.

Table 4 shows some characteristics of the PARAFAC models obtained for each of the five compounds. The third dimension of the data tensors was comprised of 10 calibration standards, the 6 samples to evaluate repeatability, 2 samples corresponding to the measure of the empty headspace vials, 8 water samples (M1 and M2), another empty headspace vial measured at the end of all the experimentation and the rest were food simulant samples that came from the migration testing performed on nylon spoons except for the case of 3C4FA in which the last sample of its data tensor corresponded to a sample with 10 μg L^{-1} of all the analytes to provide a greater variation of this analyte. It was checked that there was not memory effect. There were not shifts in the retention time of aniline and the interferent that coeluted with this analyte was better separated in these samples so a coherent two-factor PARAFAC model was obtained. However, it was only necessary to consider the first 5 scans for the data tensor of 3C4FA (those in which the analyte is found mostly) to obtain a coherent two-factor PARAFAC model.

The identification of the analytes, according to the relative abundance of the *m/z* ratios recorded (see the last column of Table 6) and the retention time, was satisfactory for all the compounds analyzed according to legislation [54,55].

For each analyte, a LS regression model between the “standardized loadings of the sample profile *versus* true concentration” was performed. Three outliers were detected using a least median of squares (LMS) regression [41,58] for 2,4-TDA (standards with concentrations of 7, 10 and 13 μg L^{-1}) and for 4,4’-MDA (standards with concentrations of 4, 10 and 13 μg L^{-1}), whereas there were not outliers in the regression model for aniline. After the elimination of the outliers, a new LS regression was estimated and validated with the rest of the data. The accuracy line was used to calculate the figures of merit. Furthermore, the trueness of the method was verified for all the analytes at the 95% significance level. Table 8 shows the parameters of the regression models performed for each case and some of the figures of merit obtained. To calculate the values of the mean absolute of the relative error, the samples with calculated concentrations higher than CCβ were only considered; so the values obtained were 3.26 % (n=6) for A, 10.46 % (n=3) for 2,4-TDA and 2.94 % (n=3) for 4,4’-MDA. The values for the capability of detection (CCβ), for a probability of false positive and false negative fixed at 0.05, were 2.09 μg L^{-1} for A, 2.36 μg L^{-1} for 2,4-TDA and 1.59 μg L^{-1} for 4,4´-MDA. These values of CCα and CCβ obtained with the optimized procedure were lower than the ones obtained in the calibration performed before the optimization step (see section 4.2, Table 7). The best improvement was obtained for 4,4’-MDA.

The repeatability of the method for each analyte was calculated as the standard deviation of the calculated concentration of the six repeatability samples measured, so the values

ACCEPTED MANUSCRIPT

obtained were 1.12 μg L^{-1} for A, 1.04 μg L^{-1} for 2,4-TDA and 1.68 μg L^{-1} for 4,4'-MDA. The repeatability expressed as the coefficient of variation (CV) was 20.89 %, 17.82 % and 23.64 %, respectively. When these values are taken into account, it can be concluded that this low precision is due to the derivatization reaction procedure and the condition of the fiber at each moment.

4.4.2. Identification and quantification of PAAs in water samples

Two water samples (M1 and M2) were analyzed following the optimized procedure. A blank and three spiked samples at three levels of concentration (1, 7 and 13 μg L^{-1} of A, 2,4-TDA and 4,4'-MDA) were measured for each water sample. The concentration of the two internal standards was fixed at 1 μg L^{-1}. Samples 19 and 23 of the PARAFAC decompositions obtained for all the studied compounds corresponded to the reagent blank sample which only contained the internal standards and the three fortified water samples were the following three samples (from 20 to 22 for M1 and samples 24 to 26 for M2).

All the samples included in these data tensors were measured with the same fiber, except for the water samples because the fiber resists a limited number of punctures. The behaviour of both fibers is different, as it can be clearly seen in Fig. 5(d), in which the sample loadings of the interferent remain constant expect for samples 19 to 26 (water samples) in which they are lower. Furthermore, although the loadings for some of the spiked water samples were lower than those corresponding to the calibration (difference that may be due to the utilization of another fiber), these discrepancies disappear when those values are standardized by the loadings of its IS.

The confidence intervals at 95% confidence level of the calculated concentrations for the blank sample of M1 were: (-1.44, 1.24) μg L^{-1} for A, (-1.23, 1.92) μg L^{-1} for 2,4-TDA and (-0.25, 1.84) μg L^{-1} for 4,4'-MDA. These concentration values are statistically equal to zero. The same conclusion is obtained for the calculated concentrations of the blank sample of M2; therefore, it can be concluded that none of the PAAs studied in this work were detected in the two water samples analyzed.

Table 9 shows the estimated concentrations for the two water samples together with the corresponding absolute values of the relative errors in prediction. The spiked samples at 1 μg L^{-1} have not been quantified because this concentration is below the CCβ of the three analytes. The spiked sample at 7 μg L^{-1} was an outlier for 2,4-TDA and 4,4'-MDA. The relative errors obtained were satisfactory; particularly for A and 2,4-TDA (values between 4.95 and 18.80, except for one case).

4.4.3. Analysis in food simulant samples: migration from black nylon spoons

The migration of PAAs from four black nylon spoons into food simulant B was studied through the optimized procedure. High amounts of some of the PAAs studied in this work were detected in some of the spoons so a dilution of the migration solutions was necessary prior to analysis. Thus, two dilutions were necessary for simulant from spoon 2: one of them to quantify 4,4'-MDA (diluted 2000 times) and the other to detect the aniline migrated (diluted

ACCEPTED MANUSCRIPT

100 times), simulant from spoon 3 was diluted 8000 times; whereas the simulants from spoon 1 and 4 were not diluted.

Three non-spiked and other three spiked food simulant samples (4 μg L^{-1} of A, 2,4-TDA and 4,4'-MDA; internal standards at 1 μg L^{-1}) were analyzed for the simulant (or its dilution) obtained from the migration test and they were also analyzed for the simulant obtained at the migration test conditions that has not been into contact with a spoon. The derivatization reaction was carried out for these 36 samples in the same way as in Section 2.3.1.

The data tensors built for A, 2,4-TDA and 3C4FA contained these 36 simulant samples together with the samples detailed in the previous Section 4.4.1. However, the data tensors for 2ABP and 4,4'-MDA contained 30 simulant samples because the ones from spoon 2 diluted 100 times were not included due to the high content of 4,4'-MDA. The last sample of the tensor for aniline corresponded to a simulant sample from spoon 3 (diluted 100 times) with the aim of being able to identify aniline. The characteristics of the PARAFAC decompositions performed are collected in Table 4.

By way of example, the sample loadings for A and its interferent are represented in Fig. 5 (d). The empty headspace vials measured correspond to samples 1, 18 and 63. The loadings of the interferent and of aniline are zero in samples 1, 18 and 63; therefore, the interferent does not appear in the empty headspace vials (it cannot be due to the fiber or instrument) and there is not memory effect. Therefore, that interferent seems to be possibly related to the derivatization reaction. The loading of aniline in sample 64 is different from zero so aniline was detected and unequivocally identified in spoon 3. Aniline also appears in spoon 2 (see the loadings for the non-spiked samples of the simulant from spoon 2 in Fig. 5 (d)). As can be seen in this figure, the sample loadings of some calibration standards are not in increasing order, however, the variations in the chromatographic signals are corrected when the loadings are standardized. The analyte 2,4-TDA has this same behaviour.

Table 10 collects the calculated concentrations for each food simulant sample analyzed together with the recovery rates obtained. The analyte 2,4-TDA was not detected in any case (the confidence intervals at 95% confidence level for the non-spiked samples contained zero). Aniline was only detected in spoon 2 (diluted 100 times) and in spoon 3 but its quantification was not possible. However, the analyte 4,4'-MDA was detected in the spoons 2,3 and 4. Bearing in mind the dilution factor and the recovery rate, the average 4,4'-MDA concentration migrated to the simulant was: 3030 ± 284 μg L^{-1} from spoon 2 and 0.63 ± 0.37 μg L^{-1} from spoon 4. The recovery rate for spoon 3 was not acceptable so, although 4,4'-MDA was detected, the final value of its concentration in the simulant was not provided. The high migration of 4,4'-MDA found in spoon 2 exceeds the permitted limit established by regulation [11] (10 μg kg^{-1}) more than 300 times; whereas the amount found in spoon 4 is below this limit.

The recovery rates obtained may be due to several aspects: the affinity of the fiber with 4,4'-MDA in this work is higher than for the other analytes. If the simulants contain high amounts of this analyte, the rest of the analytes will be less adsorbed by the fiber and worst results will be obtained; for example for spoon 2 and 3. In fact, this effect is clearly seen in the simulant from spoon 2 diluted 100 times which contains a high amount of 4,4'-MDA. In this particular case, the internal standard (3C4FA) has been practically lost due to the competition of the analytes for the sites in the fiber so the results were not acceptable and

ACCEPTED MANUSCRIPT

the quantification was not possible in this case. However, the results obtained for spoon 1, in which the migration was lower, are better. Keeping in mind that this procedure is affected by several sources of variability (the derivatization reaction and the fiber) in addition to the one caused by the instrument, it can be concluded that the recovery rates obtained were coherent with the procedure.

5. Conclusions

The derivatization reaction of PAAs prior to determination described in this work makes possible the analysis by means of HS-SPME-GC/MS. The use of a D-optimal design, together with PARAFAC, in the optimization of the HS-SPME procedure and of the derivatization reaction has enabled to carry out this optimization without the need to perform a calibration in each experimental condition. In fact, considering 7 levels of calibration and the 10 experiments plus 2 replicates measured in the optimization step; the number of runs has been reduced from 86 to 19. Therefore, the above procedure saves costs and lengthens the life of the fiber used.

The problems due to the shifts in the retention time for some of the analytes were solved by the use of GC/MS three-way data and PARAFAC2 decomposition, even in the presence of coeluting interferents. Moreover, PARAFAC and PARAFAC2 models have helped to overcome problems when some m/z ions of the analyte of interest are shared with the interferent. In addition, the unequivocal identification and quantification of each analyte according to the requirements established by regulations were possible using a PARAFAC or PARAFAC2 decomposition. In consequence, false non-compliant and false compliant results are also avoided.

The procedure developed cannot be applied when the 4,4'-MDA concentration is high and/or other interferents have migrated from the nylon spoons to the food simulant because there is a competing effect in the fiber due to other analytes that come from the matrix. However, the results obtained for the water samples were satisfactory. The predominant analytes found in the food simulants analyzed were aniline and 4,4'-MDA.

6. Acknowledgments

The authors thank the financial support provided by projects of the Ministerio de Economía y Competitividad (CTQ2011-26022) and Junta de Castilla y León (BU108A11-2). L. Rubio is particularly grateful to Universidad de Burgos for her FPI grant.

7. References

FIGURE CAPTIONS

Fig. 1 Total ion chromatogram (TIC) for primary aromatic amines after derivatization to the corresponding iodinated derivatives.

ACCEPTED MANUSCRIPT

— empty headspace vial; — blank; — 7 μg L^{-1} of A, 2,4-TDA and 4,4'-MDA and 1 μg L^{-1} ISs; — 7 μg L^{-1} of A, 2,4-TDA and 4,4'-MDA and 3 μg L^{-1} ISs; — 13 μg L^{-1} of A, 2,4-TDA and 4,4'-MDA and 1 μg L^{-1} ISs.

Fig. 2 Loadings of the chromatographic mode of the: a) one-factor PARAFAC model and b) PARAFAC2 model with one factor performed with the data tensor that contains the reference samples used for aniline.

Fig. 3 PARAFAC model with two factors for the data tensor of 3C4FA (internal standard) built for the calibration performed before the optimization step (blue: 3C4FA; green: interferent). a) Loadings of chromatographic mode, b) Loadings of spectral mode, c) Loadings of sample mode (sample 1: empty headspace vial, sample 2: blank, sample 3 to 8: calibration standards).

Fig. 4 Graphic analysis of the effects of the factors on the quantity extracted of each analyte according to presence–absence model of Eq. (8). Dash-dotted lines indicate the critical values beyond which factors are significant at 95% confidence level.

Fig. 5 PARAFAC model with two factors for the data tensor of aniline built with the samples analyzed in the optimal conditions (aniline: blue, interferent: purple). a) Loadings of the chromatographic mode, b) Spectral profile of aniline, c) Spectral profile of the interferent, d) Loadings of the sample profile. Aniline is represented with filled blue circles and the interferent is marked with empty purple circles. Green arrows mark the empty headspace vials and the red arrow indicates the simulant sample diluted 100 times from spoon 3. Spoon 2: simulant samples diluted 2000 times from spoon 2. (For interpretation of the references to colour in this figure legend, the reader is referred to the web version of this article).

ACCEPTED MANUSCRIPT

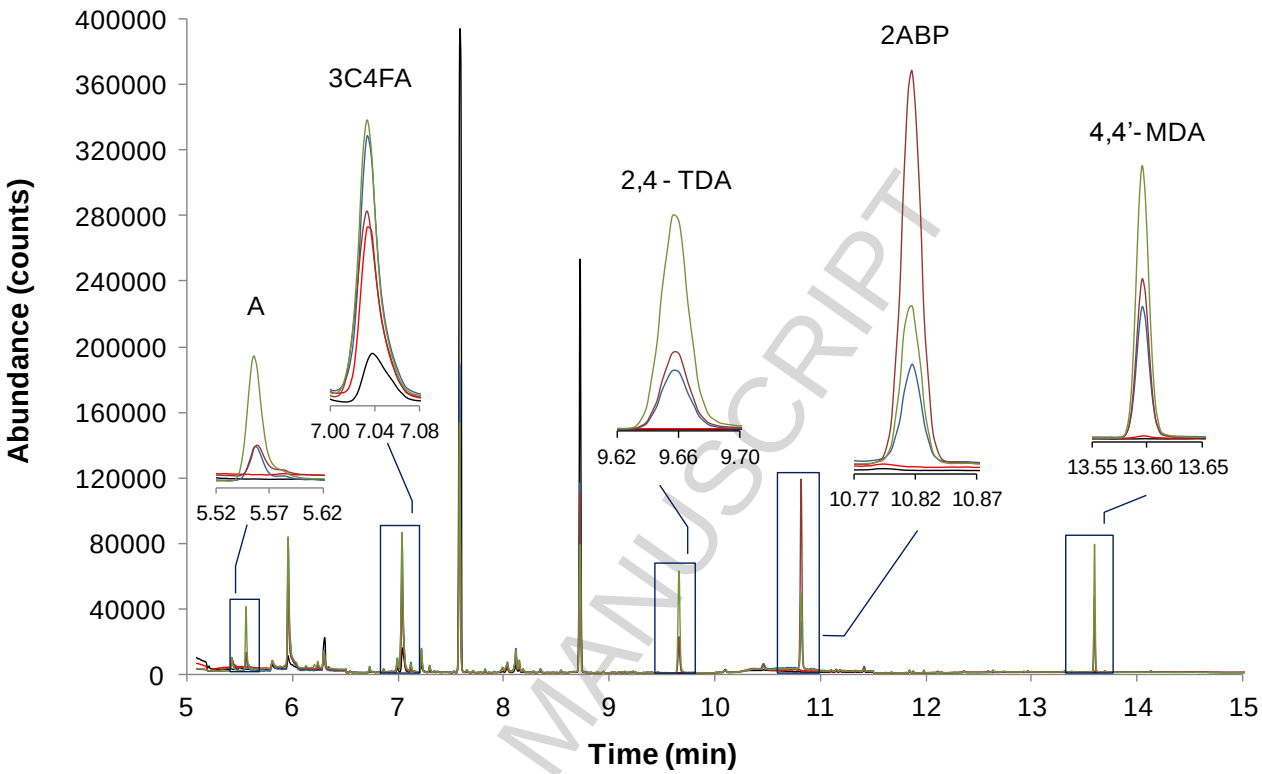

Fig. 1

ACCEPTED MANUSCRIPT

ACCEPTED MANUSCRIPT

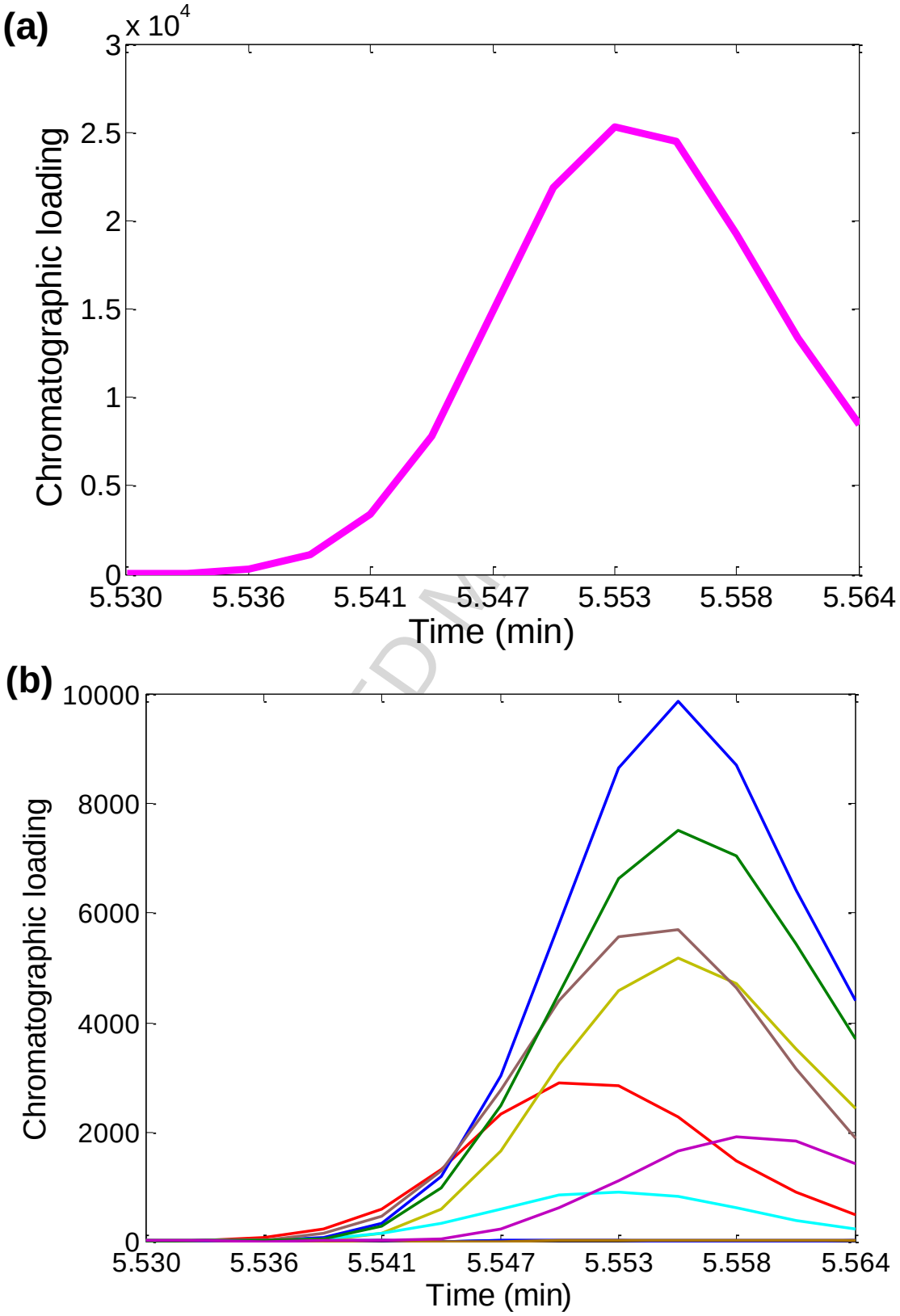

-

Fig. 2

ACCEPTED MANUSCRIPT

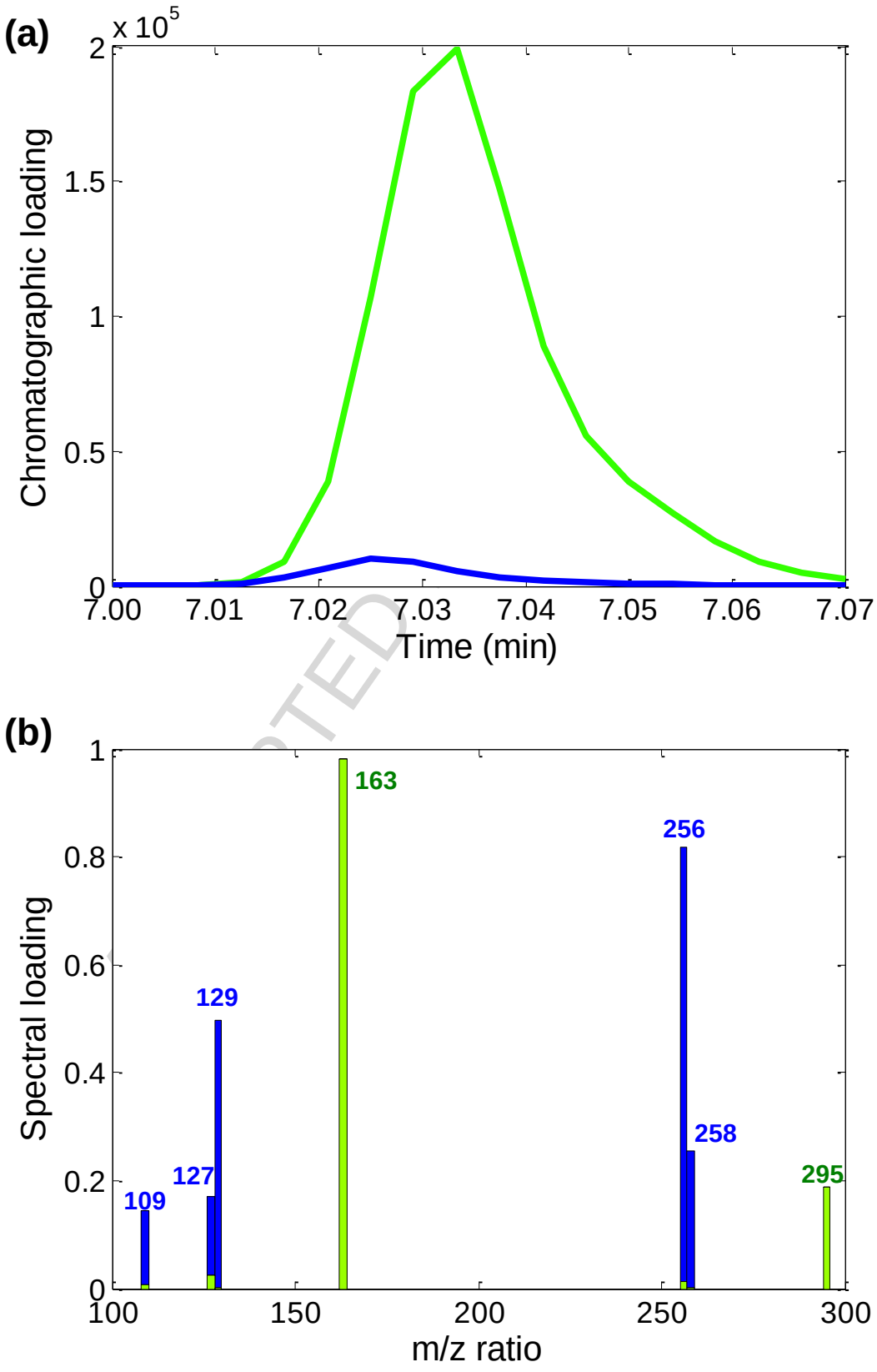

ACCEPTED MANUSCRIPT

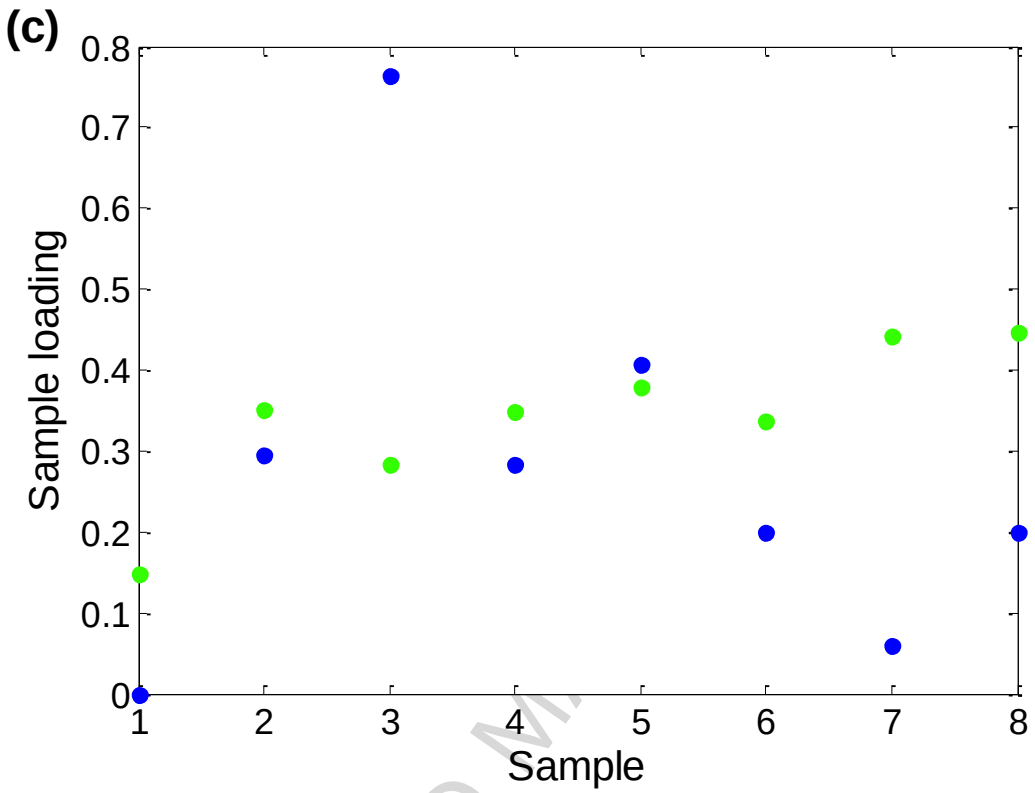

Fig. 3

ACCEPTED MANUSCRIPT

ACCEPTED MANUSCRIPT

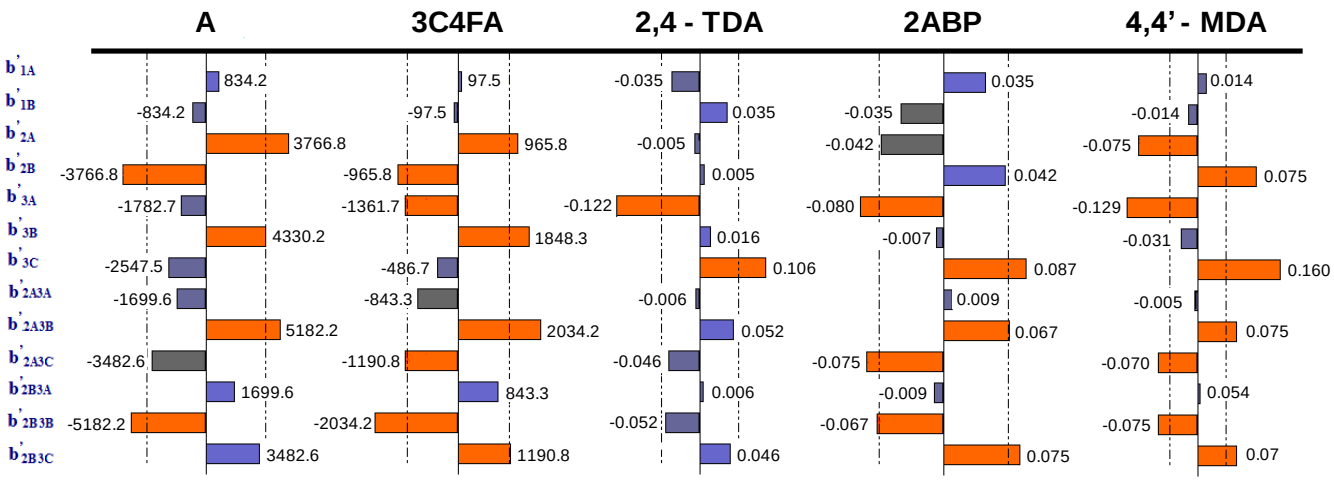

Fig. 4

ACCEPTED MANUSCRIPT

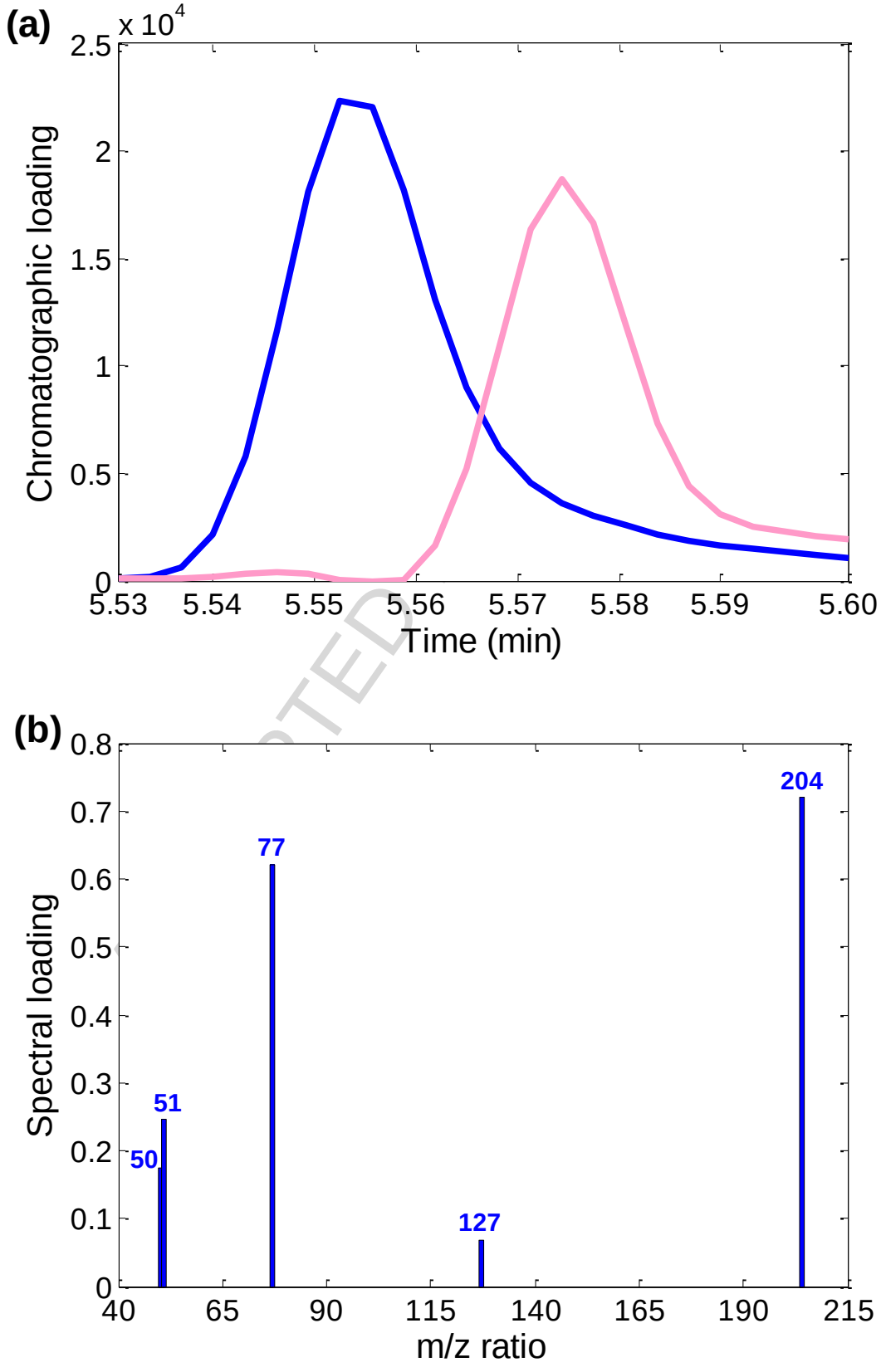

ACCEPTED MANUSCRIPT

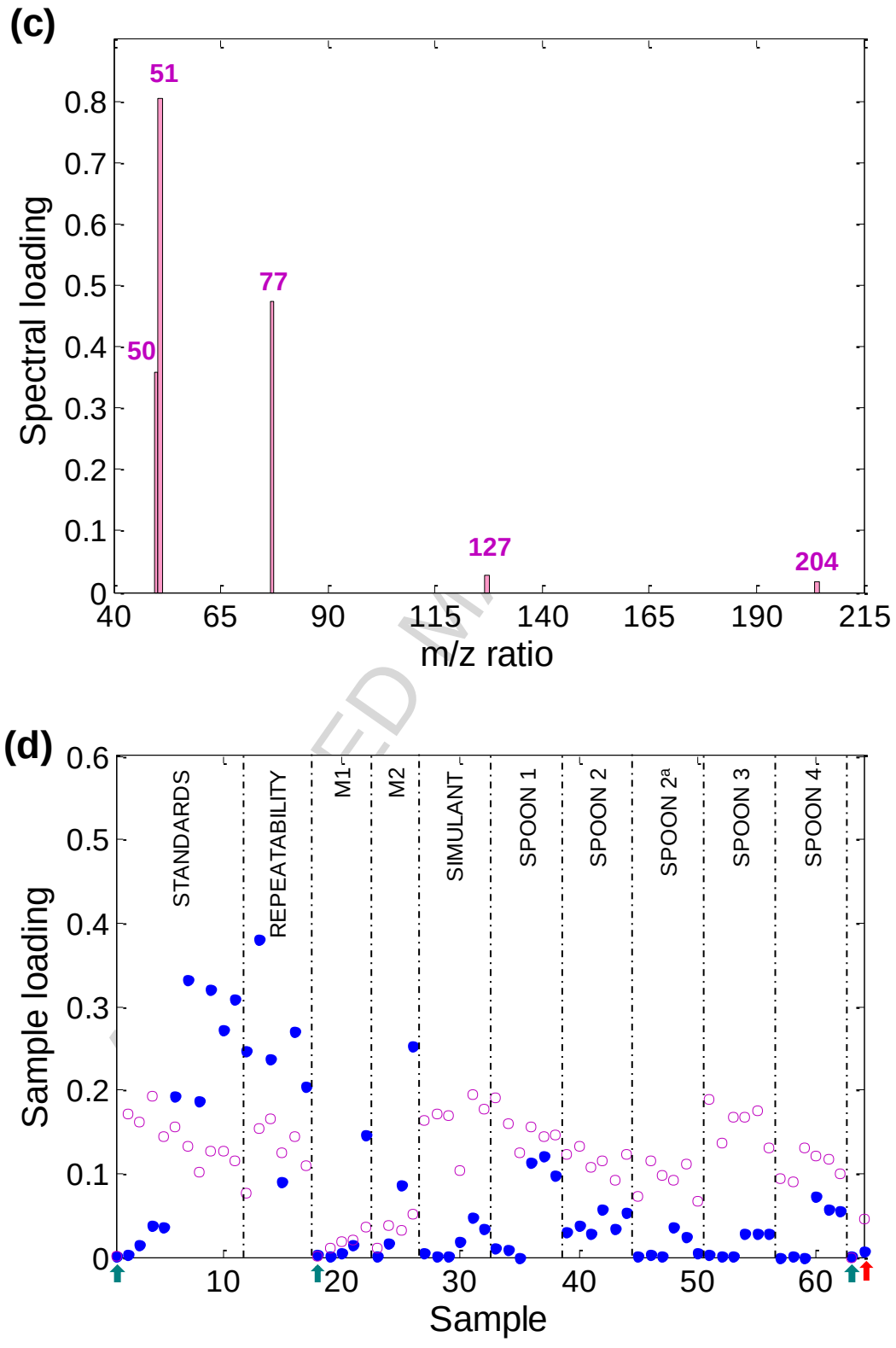

Fig. 5

ACCEPTED MANUSCRIPT

Table 1
Chemical compounds with name, chemical structure, abbreviations, their iodinated derivatives, retention time and masses used for detection.

Name	Chemical structure	Abbrev	Derivative	Chemical structure	t_R (min)	Diagnostic ions m/z[a]
Aniline	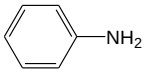	A	Iodoaniline	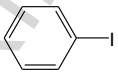	5.55	50, 51, 77, 127, **204**
3-chloro-4-fluoroaniline	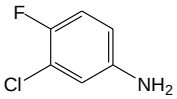	3C4FA	2-chloro-4-iodo-1-fluorobenzene	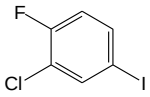	7.02	109, 127, 129, **256**, 258
2,4-diaminotoluene	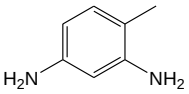	2,4-TDA	2,4-diiodotoluene	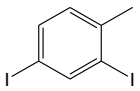	9.66	90, 127, 202, 217, 329, **344**
2-aminobiphenyl	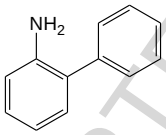	2ABP	2-iodobiphenyl	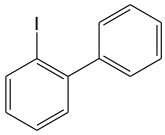	10.82	76, 127, 151, 152, 153, **280**
4,4'-diaminodiphenylmethane	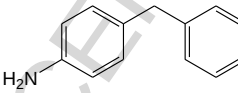	4,4´-MDA	4,4'-diiododiphenylmethane	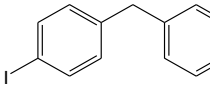	13.60	90, **165**, 217, 293, 420

[a] Base peaks are shown in bold.

ACCEPTED MANUSCRIPT

ACCEPTED MANUSCRIPT

Table 2
Factors and experimental domain for the optimization of the HS-SPME process and of the derivatization step.

Factors	Codified variable	Level A	Level B	Level C
Derivatization reaction time (min)	x_1	20	25	—
Extraction temperature in the HS (ºC)	x_2	50	65	—
Extraction time in the HS (min)	x_3	20	25	30

ACCEPTED MANUSCRIPT

ACCEPTED MANUSCRIPT

Table 3
Experimental plan and response of the D-optimal design for the optimization of the HS-SPME process and of the derivatization step for each of the three analytes (A, 2,4-TDA and 4,4'-MDA) and the two internal standards (2ABP and 3C4FA).

Run	Derivatization Reaction time(min)	Extraction temperature in the HS (ºC)	Extraction time in the HS (min)	Response (loadings of the sample mode)				
				A	2,4-TDA	2ABP	4,4'-MDA	3C4FA
1	20	50	20	7639	0.0126	0.1191	0.0242	1580
2	25	50	20	6821	0.1065	0.1043	0.0281	1510
3	20	65	20	4355	0.0353	0.2149	0.2372	1460
4	25	65	20	1836	0.1287	0.1443	0.1366	1140
5	20	50	25	21059	0.2447	0.3048	0.1981	7730
6	25	50	25	6493*	0.2674	0.1805	0.2108	2320*
7	20	65	25	3161	0.1273	0.2290	0.2177	1730
8	25	65	25	11350*	0.6254*	0.4667*	0.5242*	4120*
9	20	50	30	28857*	0.4899*	0.4335*	0.2622	8870*
10	20	50	30	7160	0.2478	0.2600	0.2942	2700
11	20	50	30	3873	0.1783	0.1995	0.2361	1640
12	20	65	30	4948	0.3143	0.4657	0.5538	2620

* Outlier datum

ACCEPTED MANUSCRIPT

ACCEPTED MANUSCRIPT

Table 4
Number of factors, data tensor size, explained variance (%) and CORCONDIA index (%) of the PARAFAC models performed for each analyte from: i) the reference samples, ii) the calibration samples analyzed before the optimization step, iii) the D-optimal design samples and iv) calibration standards + repeatability samples + water samples + food simulant samples analyzed in the optimal conditions.

Study	Analyte	Factors	Data tensor dimension[a] *I* x *J* x *K*	Explained variance (%)	CORCONDIA Index (%)
Reference samples	A	1[c]	13 × 5 × 10	99.53	—[b]
	3C4FA	2	18 × 7 × 11	98.49	100
	2,4-TDA	1	24 × 6 × 11	97.78	—[b]
	2ABP	1	27 × 6 × 11	98.65	—[b]
	4,4´-MDA	1	21 × 5 × 11	91.07	—[b]
Calibration before the optimization step	A	1[c]	13 × 5 × 8	99.58	—[b]
	3C4FA	2	18 × 7 × 8	99.56	99
	2,4-TDA	1	24 × 6 × 8	99.29	—[b]
	2ABP	1	27 × 6 × 8	99.41	—[b]
	4,4´-MDA	1	21 × 5 × 8	97.92	—[b]
D-optimal design	A	1[c]	13 × 5 × 15	99.44	—[b]
	3C4FA	2[c]	18 × 7 × 17	96.78	100
	2,4-TDA	1	24 × 6 × 15	99.31	—[b]
	2ABP	1	27 × 6 × 15	99.41	—[b]
	4,4´-MDA	1	21 × 5 × 15	98.44	—[b]
Calibration standards + repeatability samples + water samples + food simulant samples analyzed in optimal conditions	A	2	24 × 5 × 64	97.89	100
	3C4FA	2	5 × 7 × 64	99.88	100
	2,4-TDA	1	24 × 6 × 63	98.79	—[b]
	2ABP	1	27 × 6 × 57	98.92	—[b]
	4,4´-MDA	1	21 × 5 × 57	96.74	—[b]

[a] *I* refers to the number of scans, *J* refers to the number of ions recorded, and *K* refers to the number of samples.
[b] There is not CORCONDIA index in PARAFAC decomposition with only one factor.
[c] PARAFAC2 model.

ACCEPTED MANUSCRIPT

Table 5
CORCONDIA index (%) and explained variance (%) of the PARAFAC and PARAFAC2 models for aniline from: i) the reference samples, ii) the calibration samples analyzed before the optimization step and iii) the D-optimal design samples. $cos(\mathbf{a}_1,\mathbf{a}_2)$, $cos(\mathbf{b}_1,\mathbf{b}_2)$ and $cos(\mathbf{c}_1,\mathbf{c}_2)$ are the cosines between the chromatographic, spectral and sample loadings of two factors, respectively.

	PARAFAC model 1 factor		PARAFAC model 2 factors					PARAFAC2 model 1 factor	
Study	CORCONDIA Index (%)	Explained variance (%)	CORCONDIA Index (%)	Explained variance (%)	$cos(\mathbf{a}_1,\mathbf{a}_2)$	$cos(\mathbf{b}_1,\mathbf{b}_2)$	$cos(\mathbf{c}_1,\mathbf{c}_2)$	CORCONDIA Index (%)	Explained variance (%)
Reference samples	— [a]	97.06	72	99.82	0.4926	0.9832	0.8685	— [a]	99.53
Calibration before the optimization step	— [a]	98.69	74	99.92	0.4825	0.9788	0.9491	— [a]	99.58
D-optimal design	— [a]	97.96	71	99.76	0.5039	0.9736	0.8990	— [a]	99.44

[a] There is not CORCONDIA index in PARAFAC decomposition with only one factor

ACCEPTED MANUSCRIPT

Table 6
Diagnostic ions (m/z), relative abundance and tolerance intervals for the diagnostic ions for reference samples of the five PAAs and relative abundances calculated with the loadings of the spectral profiles of the PARAFAC or PARAFAC2 models performed from: i) the calibration samples analyzed before the optimization step, ii) samples of the D-optimal design and iii) calibration standards + repeatability samples + water samples + food simulant samples analyzed in optimal conditions. Ions considered to be base peaks are shown in bold. Abundances that are not within the permitted tolerances are shown in red.

Analyte	m/z	Reference samples		Initial calibration	D-optimal design	Quantitative determination in optimal conditions
		Relative abundance (%)	Tolerance interval (%)	Relative abundance (%)	Relative abundance (%)	Relative abundance (%)
A	50	22.96	[19.51 - 26.40]	23.63	21.34	24.13
	51	31.57	[26.83 - 36.31]	32.93	29.52	34.16
	77	83.01	[74.71 - 91.31]	84.88	81.63	86.39
	127	9.30	[4.65 - 13.95]	9.43	9.17	9.50
	204	100.00	—	100.00	100.00	100.00
3C4FA	109	15.34	[12.27 - 18.41]	17.08	14.37	15.88
	127	9.53	[4.77 - 14.30]	17.85	7.66	8.52
	129	65.65	[59.09 - 72.21]	61.72	62.22	62.96
	256	100.00	—	100.00	100.00	100.00
	258	31.67	[26.92 - 36.42]	31.38	32.04	31.07
2,4-TDA	90	43.42	[36.91 - 49.93]	42.56	39.12	42.38
	127	8.49	[4.25 - 12.74]	8.42	7.15	8.15
	202	0.02	[0.01 - 0.03]	0.02	0.02	0.02
	217	24.03	[20.43 - 27.63]	23.78	22.09	22.80
	329	0.06	[0.03 - 0.09]	0.08	0.08	0.19
	344	100.00	—	100.00	100.00	100.00
2ABP	76	15.88	[12.70 - 19.06]	13.61	10.54	15.78
	127	8.47	[4.24 - 12.71]	8.24	8.06	8.81
	151	26.63	[22.64 - 30.62]	26.13	24.88	26.85
	152	90.10	[81.09 - 99.11]	90.55	88.41	92.89
	153	54.82	[49.34 - 60.30]	56.03	54.86	57.01
	280	100.00	—	100.00	100.00	100.00
4,4´-MDA	90	13.87	[11.10 - 16.64]	13.69	13.89	14.14
	165	100.00	—	100.00	100.00	100.00
	217	7.56	[3.78 - 11.34]	7.35	7.36	7.42
	293	26.65	[22.65 - 30.65]	26.38	27.03	26.69
	420	77.71	[69.94 - 85.48]	77.06	84.42	82.45

ACCEPTED MANUSCRIPT

Table 7
Parameters of regression line "standardized loadings *vs* true concentration" and accuracy line "calculated concentrations *vs* true concentration": intercept, slope, standard deviation of regression (s_{yx}) and correlation coefficient for the calibration performed before the optimization step. Decision limit (CCα) and capability of detection (CCβ) at $x_0 = 0$. Probabilities of false positive and false negative fixed at 0.05.

		A	**2,4-TDA**	**4,4'-MDA**
Regression parameters "standardized loadings *vs* true concentration"	Intercept	-2245.34	-0.1291	-0.0686
	Slope	7845.99	0.3069	0.1711
	s_{yx}	5638.43	0.2185	0.1657
	Correlation coefficient	0.992	0.992	0.986
Regression parameters "calculated concentrations *vs* true concentration"	Intercept	-3.02×10^{-7}	-2.41×10^{-4}	-7.38×10^{-4}
	Slope	0.9999	0.9999	0.9999
	s_{yx}	0.7186	0.7124	0.9697
	Correlation coefficient	0.992	0.992	0.986
	CCα (x=0) (µg L^{-1})	1.66	1.74	2.36
	CCβ (x=0) (µg L^{-1})	3.18	3.32	4.51

ACCEPTED MANUSCRIPT

ACCEPTED MANUSCRIPT

Table 8
Parameters of regression line "standardized loadings *vs* true concentration" and accuracy line "calculated concentrations *vs* true concentration": intercept, slope, standard deviation of regression (s_{yx}), correlation coefficient and error (mean absolute value of relative errors in calibration) for the calibration performed in optimal conditions. Decision limit (CCα) and capability of detection (CCβ) at $x_0 = 0$. Probabilities of false positive and false negative fixed at 0.05.

		A	**2,4-TDA**	**4,4'-MDA**
Regression parameters "standardized loadings *vs* true concentration"	Intercept	0.1698	-0.1712	-0.0978
	Slope	0.4506	0.4528	0.1883
	s_{yx}	0.2349	0.2482	0.069
	Correlation coefficient	0.995	0.994	0.998
Regression parameters "calculated concentrations *vs* true concentration"	Intercept	6.5×10^{-5}	5.13×10^{-3}	9.34×10^{-4}
	Slope	0.9998	0.9977	0.9998
	s_{yx}	0.5189	0.5436	0.3664
	Correlation coefficient	0.995	0.994	0.998
	CCα (x=0) (µg L^{-1})	1.07	1.23	0.83
	CCβ (x=0) (µg L^{-1})	2.09	2.36	1.59
	Error (%)	3.26 (n=6) [a]	10.46 (n=3) [a]	2.94 (n=3) [a]

[a] Samples with calculated concentration lower than the detection capability obtained were excluded.

ACCEPTED MANUSCRIPT

Table 9
Predicted concentrations (c_{pred}) of A, 2,4-TDA and 4,4'-MDA and error (absolute value of relative errors in prediction) for two water samples (M1 and M2).

Analyte	Water sample	Sample	Standardized loading	c_{pred} (μg L^{-1})	c_{added} (μg L^{-1})	Error (%)
A	M1	Non-spiked	0.14	-0.07	0	—
		Spiked 1	0.60	0.95	1[b]	—
		Spiked 2	3.48	7.35	7	4.95
		Spiked 3	5.31	11.40	13	12.30
	M2	Non-spiked	0.14	-0.07	0	—
		Spiked 1	1.22	2.32	1[b]	—
		Spiked 2	2.11	4.31	7	38.50
		Spiked 3	6.50	14.06	13	8.12
2,4-TDA	M1	Non-spiked	0.01	0.39	0	—
		Spiked 1	0.46	1.40	1[b]	—
		Spiked 2	5.97	13.55	7	—[a]
		Spiked 3	5.19	11.83	13	8.99
	M2	Non-spiked	0.01	0.39	0	—
		Spiked 1	0.50	1.49	1[b]	—
		Spiked 2	2.40	5.68	7	18.80
		Spiked 3	5.09	11.62	13	10.60
4,4'-MDA	M1	Non-spiked	0.06	0.82	0	—
		Spiked 1	0.17	1.43	1[b]	—
		Spiked 2	3.49	19.06	7	—[a]
		Spiked 3	3.16	17.31	13	33.15
	M2	Non-spiked	0.06	0.82	0	—
		Spiked 1	0.12	1.18	1[b]	—
		Spiked 2	1.94	10.83	7	54.74
		Spiked 3	2.94	16.15	13	24.22

[a] Outlier sample.
[b] Samples with spiked concentration lower than the detection capability obtained were excluded.

ACCEPTED MANUSCRIPT

Table 10
Food simulant samples analyzed: added concentration, concentration of A, 2,4-TDA and 4,4'-MDA predicted from the linear regression "standardized sample loading *versus* true concentration" and recovery rate (%) in each case.

	Sample	c_{added} ($\mu g\ L^{-1}$)	c_{pred} A ($\mu g\ L^{-1}$)	Recovery (%)	c_{pred} 2,4-TDA ($\mu g\ L^{-1}$)	Recovery (%)	c_{pred} 4,4'-MDA ($\mu g\ L^{-1}$)	Recovery (%)
Simulant	Non-spiked 1	0	-0.18 ± 1.34		0.39 ± 1.81		0.66 ± 1.05	
	Non-spiked 2	0	-0.27 ± 1.34		0.46 ± 1.81		0.75 ± 1.04	
	Non-spiked 3	0	-0.35 ± 1.35		0.46 ± 1.81		0.75 ± 1.04	
	Spiked 1	4	2.24 ± 1.29		7.39 ± 1.52		8.18 ± 1.05	
	Spiked 2	4	1.74 ± 1.30		4.24 ± 1.60		5.29 ± 1.01	
	Spiked 3	4	1.66 ± 1.30	46.90	4.06 ± 1.61	130.74	4.36 ± 1.01	148.53
Spoon 1	Non-spiked 1	0	-0.28 ± 1.34		0.39 ± 1.81		0.70 ± 1.04	
	Non-spiked 2	0	-0.25 ± 1.34		0.38 ± 1.81		0.71 ± 1.04	
	Non-spiked 3	0	-0.38 ± 1.35		0.39 ± 1.81		0.92 ± 1.04	
	Spiked 1	4	1.62 ± 1.30		2.19 ± 1.70		3.07 ± 1.01	
	Spiked 2	4	2.00 ± 1.29		3.35 ± 1.64		4.50 ± 1.01	
	Spiked 3	4	1.80 ± 1.30	45.18	3.72 ± 1.62	77.18	3.10 ± 1.01	88.93
Spoon 2[a]	Non-spiked 1	0	-0.14 ± 1.34		0.41 ± 1.81		7.04 ± 1.03	
	Non-spiked 2	0	0.33 ± 1.33		0.59 ± 1.80		7.62 ± 1.04	
	Non-spiked 3	0	-0.33 ± 1.35		0.45 ± 1.81		7.42 ± 1.04	
	Spiked 1	4	3.81 ± 1.27		9.40 ± 1.51		12.06 ± 1.18	
	Spiked 2	4	6.02 ± 1.26		14.91 ± 1.68		12.38 ± 119	
	Spiked 3	4	6.45 ± 1.26	135.62	21.06 ± 2.12	—[b]	—[c]	121.50
Spoon 3	Non-spiked 1	0	-0.27 ± 1.34		0.45 ± 1.81		5.55 ± 1.01	
	Non-	0	-0.32 ±		0.43 ±		6.12 ±	

ACCEPTED MANUSCRIPT

	spiked 2		1.34		1.81		1.02	
	Non-spiked 3	0	-0.34 ± 1.35		0.39 ± 1.81		4.59 ± 1.01	
	Spiked 1	4	1.91 ± 1.29		7.11 ± 1.52		12.83 ± 1.21	
	Spiked 2	4	2.08 ± 1.29		6.33± 1.53		13.52 ± 1.24	
	Spiked 3	4	1.41 ± 1.30	45.03	5.09 ± 1.57	154.40	13.04 ± 1.22	— [b]
Spoon 4	Non-spiked 1	0	-0.38 ± 1.35		0.42 ± 1.81		1.11 ± 1.04	
	Non-spiked 2	0	-0.30± 1.34		0.49 ± 1.81		1.28 ± 1.03	
	Non-spiked 3	0	-0.38 ± 1.35		0.42 ± 1.81		0.90 ± 1.04	
	Spiked 1	4	1.05 ± 1.31		3.87 ± 1.62		3.13 ± 1.01	
	Spiked 2	4	1.17 ± 1.31		5.78 ± 1.55		2.74 ± 1.01	
	Spiked 3	4	1.12 ± 1.31	27.85	7.72 ± 1.51	144.73	2.64 ± 1.01	43.42

[a] Food simulant diluted 2000 times.
[b] Recovery rate value was not acceptable.
[c] Outlier sample.

ACCEPTED MANUSCRIPT

ACCEPTED MANUSCRIPT

HIGHLIGHTS

A HS-SPME-GC/MS method was developed to determine primary aromatic amines

A D-optimal design was used to optimize the HS-SPME process and derivatization step

PARAFAC or PARAFAC2 decomposition made possible to identify unequivocally PAAs

PAAs were determined in water and in migration samples from nylon cooking utensils

Figures of merit obtained with a PARAFAC calibration for several PAAs were evaluated

[1] H. Kataoka, J. Chromatogr. A, 733 (1996) 19-34.

[2] R.D. Voyksner, R. Straub, J.T. Keever, H.S. Freeman, W.N. Hsu, Environ. Sci. Technol. 27 (1993) 1665-1672.

[3] C. Lambert, M. Larroque, J.C. Lebrun, J.F. Gerard, Food Addit. Contam. 14 (1997) 199-208.

[4] G. Lawson, C.T. Barkby, C. Lawson, Fresenius J. Anal. Chem. 354 (1996) 483-489.

[5] I.S. Arvanitoyannis, l. Bosnea, Crit. Rev. Food Sci. Nutr., 44 (2004) 63–76.

[6] G. Baughman, E.Weber, Environ. Sci. Technol. 28 (1994) 267–276.

[7] K. Marchildon, Macromol. React. Eng. 5 (2011) 22–54.

[8] United Nations Environment Programme/Organisation of Economic Co-operation and Development (UNEP/OECD). 2002. 4,4'-Methylenedianiline. Dortmund: OECD-SIDs.

[9] World Health Organization and International Agency for Research on Cancer (WHO/IARC). 2010. Monographs on the evaluation of carcinogenic risks to humans: some aromatic amines, organic dyes and related exposures. Lyon (France): IARC.

[10] International Agency for Research on Cancer (IARC). IARC Monographs on the Evaluation of Carcinogenic Risks to Humans. Available at: http://monographs.iarc.fr/ENG/Classification/ (Last update: 10/04/2013, accessed 10/07/13).

[11] European Commission. 2011. Commission Regulation (EU) 10/2011 on plastic materials and articles intended to come into contact with food. 2011. Off. J. Eur. Commun. L12 (15 January) 1–89.

[12] European Commission. 2011. Commission Regulation (EU) 16/2011 laying down implementing measures for the Rapid alert system for food and feed. Off. J. Eur. Commun. L6 (11 January) 7–10.

[13] RASFF 2012 Annual Report. Rapid Alert System for Food and Feed, European Commission, Health and Consumers. Available at: http://ec.europa.eu/food/food/rapidalert/index_en.htm (Accessed 10/07/13).

[14] RASFF Portal. See: https://webgate.ec.europa.eu/rasff-window/portal/index.cfm

ACCEPTED MANUSCRIPT

[15] X. Trier, B. Okholm, A. Foverskov, M.-L. Binderup, J. H. Petersen, Food Addit. Contam. 27 (2010) 1325–1335.

[16] A. Fekete, A.K. Malik, A. Kumar, P. Schmitt-Kopplin, Crit. Rev. Anal. Chem. 40 (2010) 102–121.

[17] R.M. Riggin, T.F. Cole, S. Billets, Anal. Chem. 55 (1983) 1862-1869.

[18] D.E. Bradway, T. Shafik, J. Chromatogr. Sci. 15 (1977) 322-328.

[19] A. Fromberg, T. Nilsson, B.R. Larsen, L. Montanarella, S. Facchetti, J.Ø. Madsen, J. Chromatogr. A 746 (1996) 71-81.

[20] C.S. Lu, S.D. Huang, J. Chromatogr. A 696 (1995) 201-208.

[21] T.D. Behymer, T.A. Bellar, W.L. Budde, Anal. Chem. 62 (1990) 1686-1690.

[22] R. Sendón, J. Bustos, J. J. Sánchez, P. Paseiro, M. E. Cirugeda, Food Addit. Contam. 27 (2010) 107–117.

[23] A. Cavallaro, V. Piangerelli, F. Nerini, S. Cavalli, C. Reschiotto, J. Chromatogr. A 709 (1995) 361-366.

[24] X. Wang, Y. Chen, J. Chromatogr. A 1216 (2009) 7324-7328.

[25] J. Zhang, X. Wu, W. Zhang, L. Xu, G. Chen, Electrophoresis 29 (2008) 796-802.

[26] A. Labudzinska, K. Gorczynska, Analyst 119 (1994) 1195-1198.

[27] C. Yu. Doronin, R.K. Chernova, N.N. Gusakova, J. Anal. Chem. 59 (2004) 335-344.

[28] H.M. Pinheiro, E. Touraud and O. Thomas, Dyes Pigm. 61 (2004) 121-139.

[29] M. Akyüz, Ş. Ata, J. Chromatogr. A, 1129 (2006) 88-94.

[30] M. Akyüz, Ş. Ata, J. Pharm. Biomed. Anal. 47 (2008) 68–80.

[31] M. Longo, A. Cavallaro, J. Chromatogr. A 753 (1996) 91-100.

[32] C. Brede, I. Skjevrak, H. Herikstad, J. Chromatogr. A 983 (2003) 35-42.

[33] L. Muller, E. Fattore, E. Benfenati, J. Chromatogr. A 791 (1997) 221-230.

[34] T.C. Schmidt, M. Less, R. Haas, E. von Löw, K. Steinbach, G. Stork, J. Chromatogr. A 810 (1998) 161.

[35] T. Zimmerman, W.J. Ensinger, T.C. Schmidt, Anal. Chem. 76 (2004) 1028-1038.

[36] Technical guidelines on testing the migration of primary aromatic amines from polyamide kitchenware and of formaldehyde from melamine kitchenware. EUR24815EN —first ed. 2011.

[37] NIST Mass Spectral Search Program for the NIST/EPA/NIH Mass Spectral Library Version 2.0 a. (build July 1 2002). National Institute of Standards and Technology, Gaithersburg, USA.

ACCEPTED MANUSCRIPT

[38] B. M. Wise, N.B. Gallagher, R. Bro, J.M. Shaver, W. Winding, R.S. Koch, PLS Toolbox 6.0.1, Eigenvector Research Inc., Manson, WA, 2008.

[39] D. Mathieu, J. Nony, R. Phan-Tan-Luu, NemrodW (Versión 2007_03), L.P.R.A.I. Marseille, France, 2007.

[40] STATGRAPHICS Centurion XVI Versión 16.1.05 (32 bit). Statpoint Technologies, Inc. 2010.

[41] P.J. Rousseeuw, A.M. Leroy, Robust Regression and Outliers Detection, John Wiley and Sons, New Jersey, 2003.

[42] L .A. Sarabia, M.C. Ortiz, Trends Anal. Chem. 13 (1994) 1-6.

[43] G.A. Lewis, D. Mathieu, R. Phan-Tan-Luu, Pharmaceutical Experimental Designs, Marcel Dekker, New York, 1999.

[44] C.A. Anderson, R. Bro, Chemom. Intell. Lab. Syst. 52 (2000) 1-4.

[45] R. Bro, Chemom. Intell. Lab. Syst. 46 (1999) 133-147.

[46] R.A. Harshman, UCLA Working Papers in Phonetics, 22 (1972) 30-47

[47] H.A.L. Kiers, J.M.F. Ten Berge, R. Bro, J. Chemom. 13 (1999) 275-294.

[48] R. Bro, C.A. Andersson, H.A.L. Kiers, J. Chemom. 13 (1999) 295-309.

[49] M.C. Ortiz, L.A. Sarabia, J. Chromatogr. A, 1158 (2007) 94–110.

[50] R. Bro, H.A.L. Kiers, J. Chemom. 17 (2003) 274–286.

[51] S. Haven, J.M.F. ten Berge, Heymans Bulletin 290 Ex. Department of Psychology, University of Groningen (1977).

[52] U. Lorenzo-Seva, J.M.F. ten Berge, European Journal of Research Methods for the Behavioral and Social Sciences, 2 (2006) 57-64.

[53] M.H. Kamstrup-Nielsen, L.G. Johnsen, R. Bro, J. Chemom. 27 (2013) 99–105.

[54] 2002/657/EC Commission Decision of 12 August 2002 implementing Council Directive 96/23/EC concerning the performance of analytical methods and the interpretation of results. Off. J. Eur. Commun. L221 (17 August) 8-36.

[55] Guidelines for performance criteria and validation procedures of analytical methods used in controls of food contact materials, EUR24105EN—first ed. 2009.

[56] M.C. Ortiz, L.A. Sarabia, A. Herrero, M.S. Sánchez, M.B. Sanz, M.E. Rueda, D. Giménez, M.E. Meléndez, Chemom. Intell. Lab. Syst. 69 (2003) 21-33.

[57] M.C. Ortiz, L.A. Sarabia, I. García, D. Gimenez, E. Meléndez, Anal. Chim. Acta 559 (2006) 124-136.

[58] M.C. Ortiz, L.A. Sarabia, A. Herrero, Talanta 70 (2006) 499-512.